A MEASUREMENT OF THE RESONANCE ESCAPE PROBABILITY OF NEUTRONS IN A HOMOGENEOUS THORIUM REACTOR

by

Lee S. Anthony

Dissertation submitted to the Graduate Faculty of

the Virginia Polytechnic Institute

in candidacy for the degree of

DOCTOR OF PHILOSOPHY

in

Physics

March 1962

Blacksburg, Virginia

II. TABLE OF CONTENTS

III. LIST OF ILLUSTRATIONS

IV. LIST OF TABLES

V. INTRODUCTION

In order to ascertain the feasibility of a proposed reactor system, and to properly design such a system with the least expenditure of time and money, it is desirable to be able to predict analytically the values of the nuclear parameters pertinent to the system. The probability of a fast neutron from the fission process surviving to thermal energies, where it may be usefully employed in a thermal reactor, is such a parameter. Since the most probable cause of absorption is interaction with materials which exhibit resonance peaks in the intermediate energy range, the above survival probability is referred to as the resonance escape probability (R.E.P.). Analytical calculations are now possible with computers, provided that the problem is not too complex either to analyze mathematically or to compute with available computing equipment. A Monte Carlo calculation has been performed at Virginia Polytechnic Institute (1) to predict the resonance escape probability in a homogeneous thorium reactor. This computation was made for low number densities of absorber, whereas most previous calculations had been performed for much higher absorber densities, such as one would encounter in fuel rods or heavy slurries. A complementary experiment was therefore performed at VPI, utilizing the Cockcroft-Walton accelerator as a source of neutrons from the $D(d,n)He^3$ reaction. This experiment investigated the resonance escape probability in the selected system as a function of absorber concentration at room temperature. The system is composed of

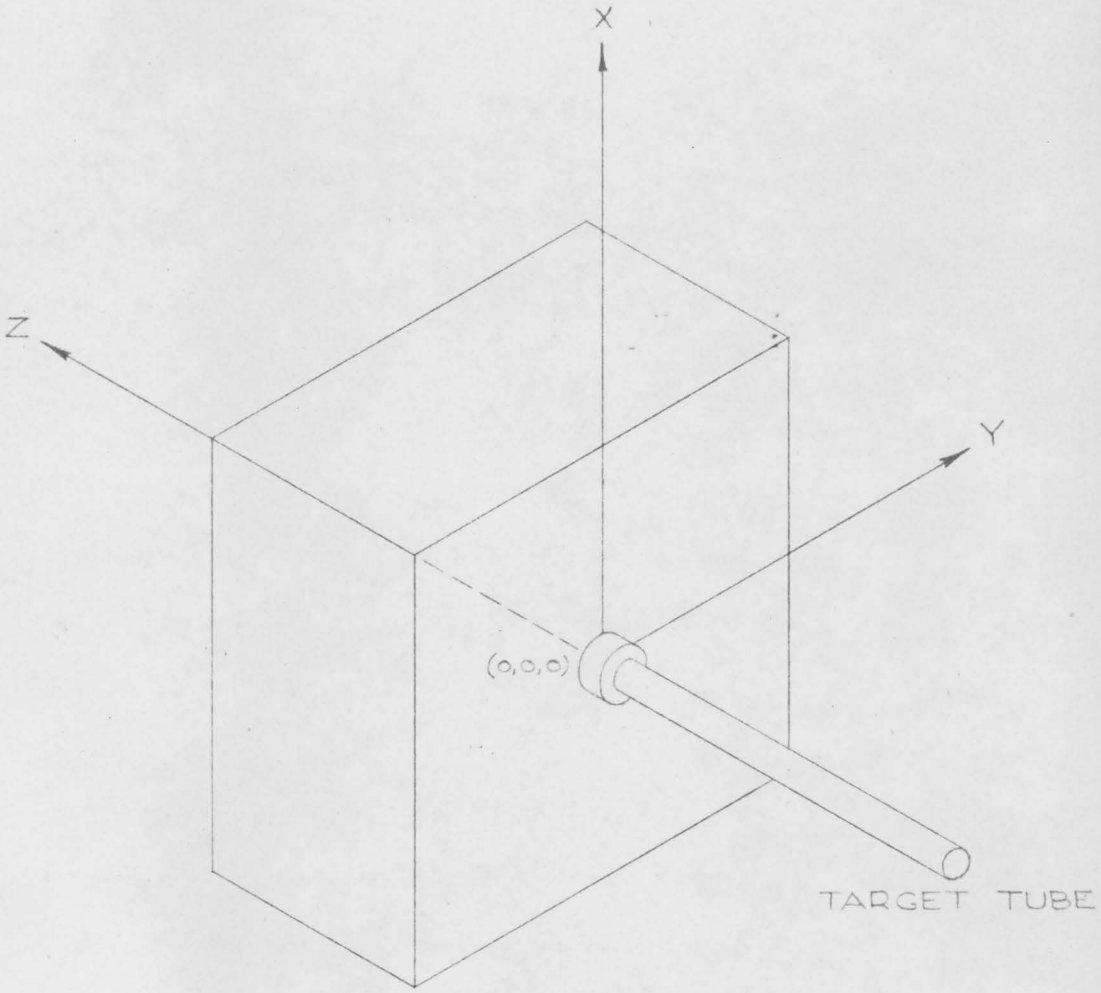

SYSTEM COORDINATES

SCALE ——————— 3/32"=1"

Fig. 1

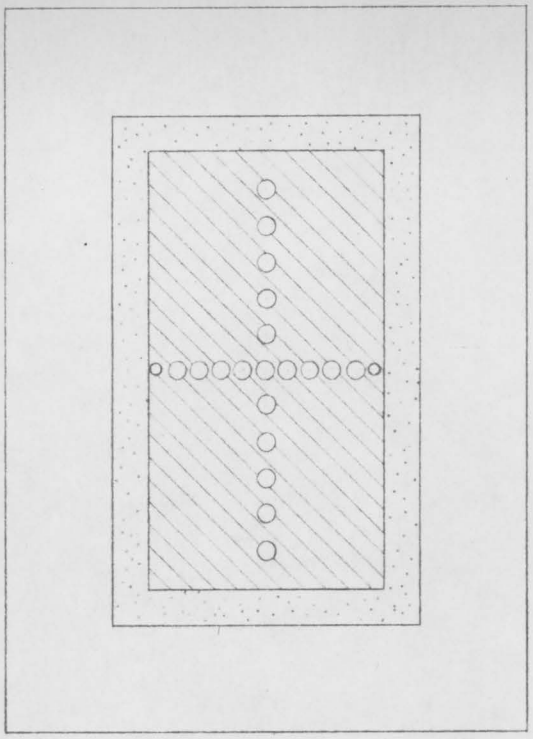

UNDERSIDE OF LID

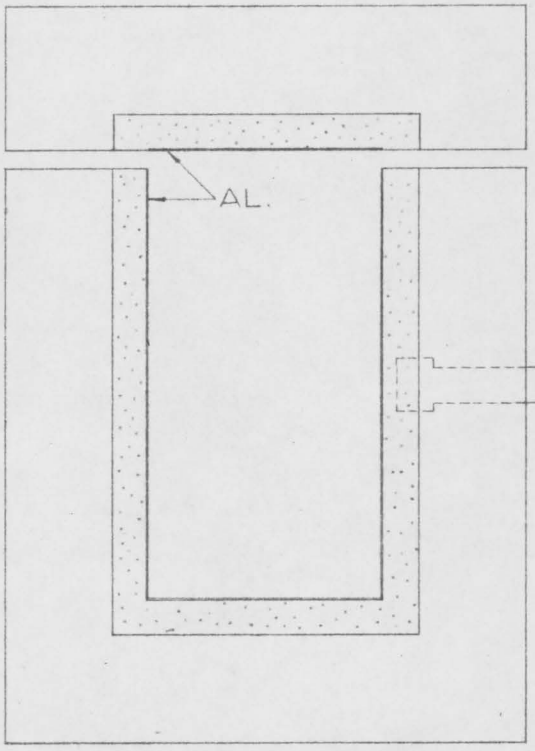

LEGEND

- PARAFFIN
- BORATED PARAFFIN
- ALUMINUM

CROSS SECTION OF SYSTEM AND LID

SCALE ——— 3/32" = 1"

Fig. 2

an aqueous solution of thorium nitrate contained in an aluminum box approximately 24" x 24" x 13". The definition of resonance escape probability used here is the ratio of neutrons which survive to 10 ev to the number which began the traversal of the resonance energy region at 1000 ev.

The experiment parallels as closely as possible the theoretical Monte Carlo analysis. A number of neutrons is introduced into the side of the box at (x = 0, y = 0, z = 0) (Fig. 1), and these are subsequently thermalized and/or absorbed in the system, or leak out of the system. The thermal neutron density in the system is sampled with a BF_3 detector. The decrease in this density upon addition of thorium nitrate is due to the combined effects of scattering and absorption with the thorium, nitrogen, and oxygen added. If one could compensate for the effect of the nitrogen, oxygen, and non-resonance absorption of thorium, then one could obtain a measure of the resonance absorption of thorium in aqueous nitrate solution. To accomplish this, iron was chosen as a material whose total cross-section closely parallels what the thorium cross-section would be without resonances. By adding the iron as ferric nitrate, the effect of nitrogen and oxygen can also be accounted for. The experiment then consisted of examining the thermal neutron density in both ferric nitrate and thorium nitrate solutions as a function of concentration, going from approximately zero concentration (pure water) to as concentrated solutions as were readily available.

In accordance with the definition of resonance escape probability given above, we would like to measure all neutrons in a given system which get to 10 ev or below. Since this is not possible, the boron detector was used because it gives a measurement of neutron density rather than flux. The difference in cross-section in this low energy range is compensated for by comparison of equivalent number densities of iron and thorium. This equivalence is based on the normalization of thermal neutron distributions in the thorium and iron systems. A measurement of neutron density in the energy range of thermal to about 0.5 ev is therefore taken as a fraction of all neutrons in the range of thermal to 10 ev.

VI. LITERATURE REVIEW

The earliest experiments to determine quantative information on the magnitude of the resonance absorption in bulk material, and its dependence on size, shape, temperature, and dilution were carried out on uranium by E. C. Creutz, R. R. Wilson, E. P. Wigner, and T. Snyder at Princeton University in 1941. These experiments, as well as theoretical work carried out in the United States during the period 1939-1941, are reported in a series of papers (2), (3), (4) in J. Appl. Phys. 26 (1955).

Activation measurements on homogeneous mixtures of uranium and various moderators were made in 1944 by Mitchell, Brown, Pruett, and Nering (5). Similar work was performed for uranium by Hughes and Goldstein (6) and for thorium by Hughes and Eggler (7).

Considerable work has also been done with ThO_2 and thorium by Dayton and Pettus, Pettus (see refs. 8, 10), and by Macklin and Pomerance (8).

Calculations pertinent to homogeneous systems have been performed by a number of people, notably Dresner (10), Nordheim (16), and Nordheim and Sampson (17).

A survey of U. S. work prior to the first Geneva Conference was reported by Macklin and Pomerance (8); a similar Russian survey was presented by Spivak et al (9). Dresner has given a very comprehensive review of the literature, theory, and experiments concerning resonance

absorption processes (10). This was published as a monograph and is the most recent summary in the field (1960). In view of the above comprehensive surveys, details of previous work are not given in this literature review.

VII. DESCRIPTION OF EXPERIMENT

An experiment was run initially to determine the effect, if any, of neutrons returning into the proposed system from the room. By placing various amounts of moderator and absorber between the target and a BF_3 detector, it was found that a considerable scatter was observed from nearby objects in the room. A shield of six inches of paraffin, two inches of borated paraffin, and a 30 mil cadmium sheet was designed to reduce the scattered neutrons. The aluminum box in which the experiment was to be run was therefore surrounded by such a shield, with the cadmium next to the box, the borated paraffin outside the cadmium, and the unborated paraffin outermost. A cross-sectional view of this system can be seen in Fig. 2.

Holes of 1-3/32" diameter were made in the lid to permit insertion of the detector.* These holes were made in two perpendicular rows, one in the beam (z) direction; the other in the (y) direction. The traversals used to determine relative neutron density were made in the (z) direction. The detector, which is cylindrical in shape, was lowered through the appropriate hole in the lid until its sensitive volume was centered at the height of the neutron target. Since the sensitive volume of the detector is approximately 10-1/2" long, the detector has some integrating action which would tend to diminish vertical inhomogenieties in the solutions.

---

*The detector was a 1/2" diameter BF_3 detector filled to 40 cm. pressure, and was manufactured by N. Wood Counter Laboratory, Chicago, Ill. The monitor was a 1" diameter BF_3 detector, type RSN-7A, ser. 556. filled to 40 cm. pressure, manufactured by Reuter-Stokes.

Another BF_3 detector was attached to the outside of the system, near the target tube, to serve as monitor. This monitor could then be used to normalize the detector readings to compensate for differing rates of neutron production. It was noted that measurement of beam current is not an exact measure of neutron production, but that the neutron production varies with accelerating voltage, beam focusing, condition of the target, and with pressure in the accelerating tube.

The target, in order to conform to the Monte Carlo conditions, was a deuterium drive-in target made of a 1/16" brass disk, and cooled by compressed air.

Counting equipment was composed of the above mentioned BF_3 detectors and two associated scalers.* The normalized measure of neutron density at a given point was expressed in terms of the ratio C2/C1. Both counting systems were checked periodically by placing the detectors in a standard geometry, which consisted of a plutonium-beryllium neutron source in a graphite pile.

The traversing detector (or detector, as opposed to the monitor), was protected from the solutions by insertion into a steel tube. It was noted that both soft solder and brass are corroded by nitrate solutions, so the tube was made by welding a steel disc on the end of a steel tube. The steel used for this purpose was type 304 stainless

---

*The scalers were Nuclear-Chicago Ultrascalers, Model 192A. The Reuter-Stokes 1" detector and Ultrascaler serial 209 are referred to as counter number one (C1); the N. Wood 1/2" detector and Ultrascaler serial 204 as counter number two (C2).

steel, and the welding was done gratis by Valley Roofing Corp., Roanoke, Virginia. Type 304 stainless steel proved resistant to corrosion by both ferric nitrate and thorium nitrate. Monel metal, which was used for fittings in the pump used for transfer and mixing of the solutions, also seemed corrosion resistant in these solutions. Nalgon plastic tubing was used in conjunction with the pump.

The aluminum box was coated inside with Miccropeel, a strippable film lacquer paint. However, the concentrated ferric nitrate solution blistered the film and caused slight localized pitting under the blisters. Before the thorium nitrate solution was run, the box was cleaned inside, and coated successively with Amercoat primer, two coats of Amercoat gray paint, and then with two coats of Miccropeel. In this case, the Miccropeel adhered well to the Amercoat and there was no evidence of blistering.

Data was characteristically taken in the following manner: the solution to be investigated was prepared by draining part of the previous solution from the box, refilling the box with demineralized water and, in the case of the viscous thorium solutions, circulating the solutions for a few hours with a pump to hasten mixing. The height of the solution in the box and the temperature of the solution were recorded, and the beam current of the accelerator was monitored and maximized. Counter efficiencies were monitored in the standard geometry, and the detectors subsequently placed in position; the monitor on the outside of the system and the detector in the solution. Traversals were normally started at one end of the 1-3/32" holes

(Fig. 2) along the (z) direction, either in position 2 or 10 (positions 1 and 11 were small holes adjacent to the edges of the system). The detector was lowered to a fixed level, at which it was symmetrically placed with respect to the target. Background counts were taken on both counters, the accelerating voltage turned on, and counting begun. After completion of a traversal, the neutron density at the initial position was re-measured to assure reproducibility of results. Normally, 10^6 counts were obtained at each point on both counters unless the counting time required for a point exceeded 5-7 hours. The count registered by the detector for a given period, corrected for resolving time, was divided by the corresponding monitor count as a means of normalization to compensate for fluctuations in neutron production. The counting rate of the monitor was sufficiently slow so that it required no resolving time corrections.

Location of the monitor was extensively investigated. The monitor was initially placed at different positions within the system and the possibility of interaction between the detector and the monitor investigated. When the monitor was placed so that its counting rate would be compatible with counting times at a given point of seven hours or less (as in position 1, near the target), there was a slight indication of a flux depression around the monitor by the detector when the detector was covered with cadmium and placed in the adjacent position. The monitor was therefore placed on the outside of the paraffin shielding, where there was no longer any such

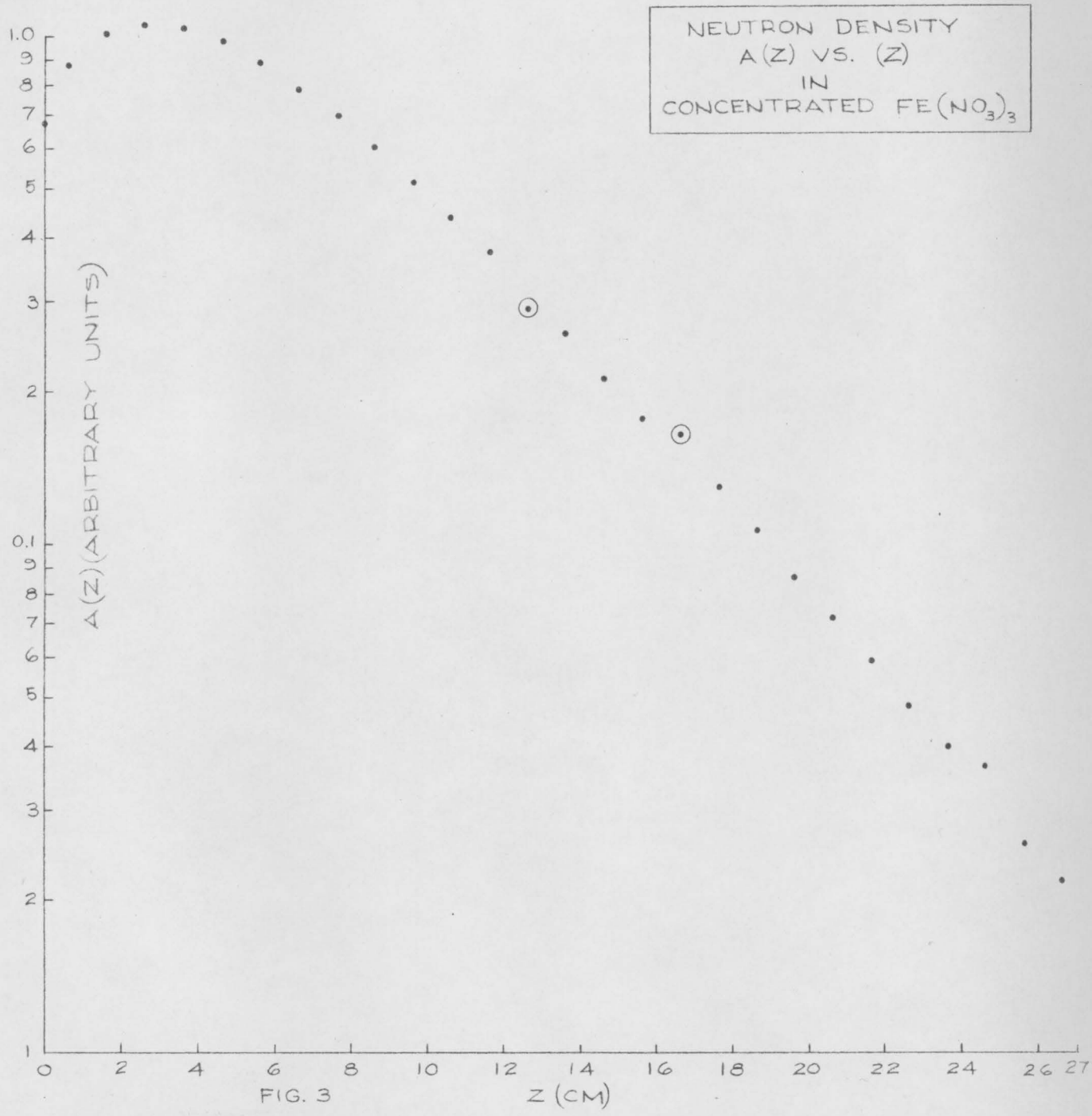
NEUTRON DENSITY
A(Z) VS. (Z)
IN
CONCENTRATED FE(NO3)3
A(Z)(ARBITRARY UNITS)
1.0
9
8
7
6
5
4
3
2
0.1
9
8
7
6
5
4
3
2
1
0
2
4
6
8
10
12
14
16
18
20
22
24
26
27
Z (CM)

FIG. 3

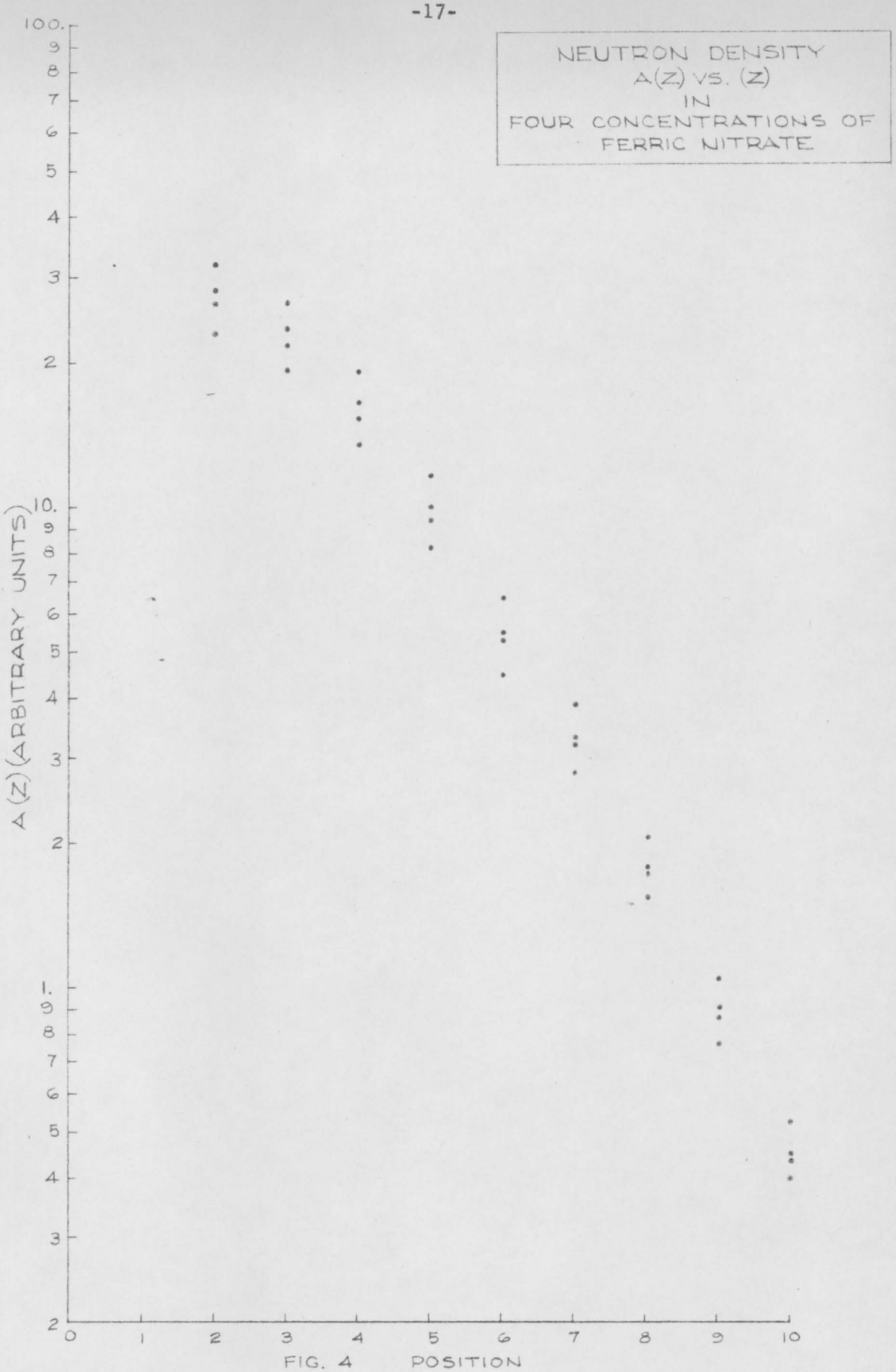
NEUTRON DENSITY
A(Z) VS. (Z)
IN
FOUR CONCENTRATIONS OF
FERRIC NITRATE
A (Z) (ARBITRARY UNITS)
100.
9
8
7
6
5
4
3
2
10.
9
8
7
6
5
4
3
2
1.
9
8
7
6
5
4
3
2
0
1
2
3
4
5
6
7
8
9
10
POSITION

FIG. 4

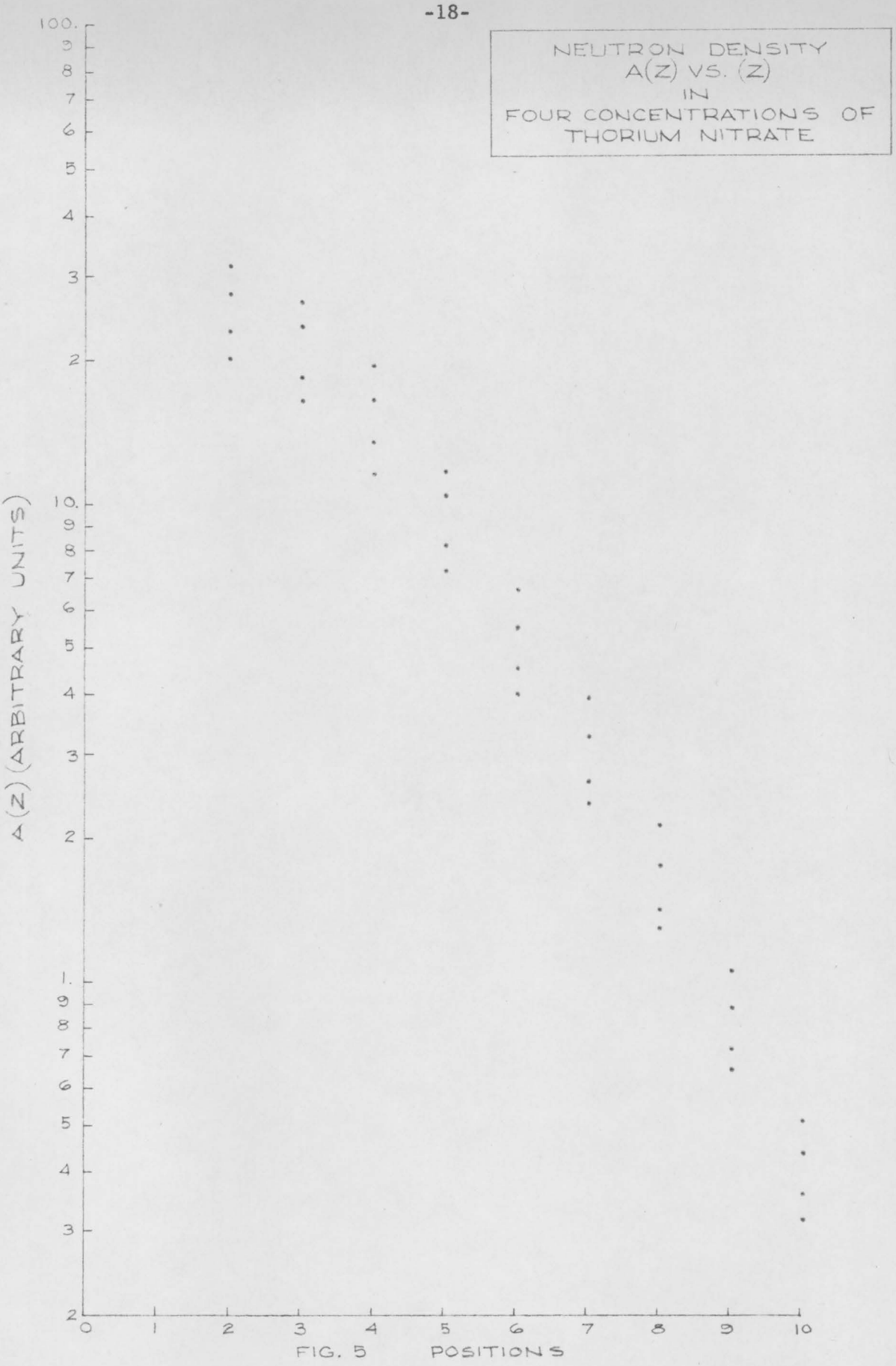
NEUTRON DENSITY
A(Z) VS. (Z)
IN
FOUR CONCENTRATIONS OF
THORIUM NITRATE
A(Z) (ARBITRARY UNITS)
100.
9
8
7
6
5
4
3
2
10.
9
8
7
6
5
4
3
2
1.
9
8
7
6
5
4
3
2
0
1
2
3
4
5
6
7
8
9
10
POSITIONS

FIG. 5

effect, even though the cadmium cover was not normally used on the detector, but only to determine flux behavior in the various solutions.

A lateral traverse (Fig. 6) was made in the (y) direction at (z = position 6) to ascertain the general shape of, and to look for, any significant irregularities in the neutron density in this region. No such irregularities were noted.

Resolving Time

The resolving time of the Nuclear-Chicago Ultrascalers was determined by introducing a series of two pulses with a variable delay between them. Both pulses were obtained from a Hewlett-Packard pulse generator, Model 212A; the primary or repetition pulse being obtained from the "sync output" and the second or delayed pulse from the "pulse output". The position in time of the second pulse with respect to the first pulse is varied by adjusting the "pulse advance" setting. These pulses were mixed in a UHF tee and fed into the input jack of the Ultrascaler. Whenever the delay between two pulses is more than the resolving time of the scaler, two pulses are counted for each two introduced into the input. Conversely, when the second pulse is introduced within the resolving time of the scaler, only one pulse is counted for each two introduced at the input. Therefore, by delaying the time interval between the two pulses and noting where the counting rate changes by a factor of two, the resolving time of the scaler is found. As may be noted in Figs. 7 and 8, the

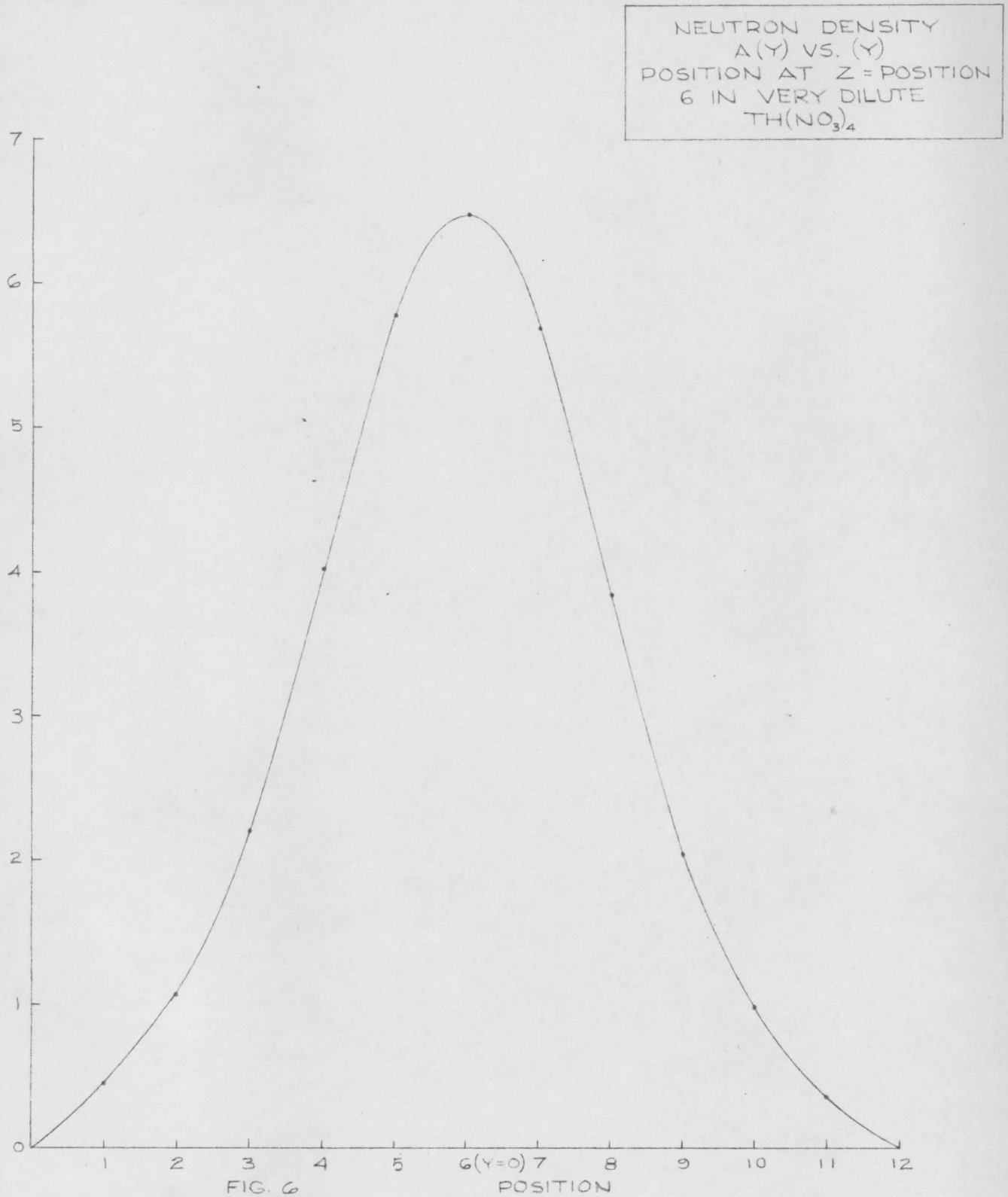
NEUTRON DENSITY
A(Y) VS. (Y)
POSITION AT Z = POSITION
6 IN VERY DILUTE
TH(NO3)4
7
6
5
4
3
2
1
0
1
2
3
4
5
6(Y=0)
7
8
9
10
11
12
POSITION

FIG. 6

resolving time was found to be approximately 5 μ sec for pulses of approximately the same size as those obtained from a BF_3 detector (i.e., of the order of 5 mv in amplitude and 2 μs wide.)

Solutions

The concentrated solution of ferric nitrate was made by dissolving two hundred pounds of Fisher certified reagent grade $Fe(NO_3)_3 \cdot 9H_2O$ crystals in water, the total volume of solution being 119,770 ± 200 cc.

Dilution were performed in the system by pumping or siphoning off part of the solution and refilling with water.

The concentrated solution of thorium nitrate was obtained from Davison Chemical Co., Erwin, Tennessee. The analysis of this solution is given in Table 8. Dilutions were performed as above with subsequent pumping of the diluted solutions to hasten mixing, since concentrated thorium nitrate is somewhat viscous.

The water used to perform these dilutions was obtained from the Barnstead demineralizer associated with the VPI reactor, and the purity of the water ranged from 0.1 - 0.5 ppm as NaCl.

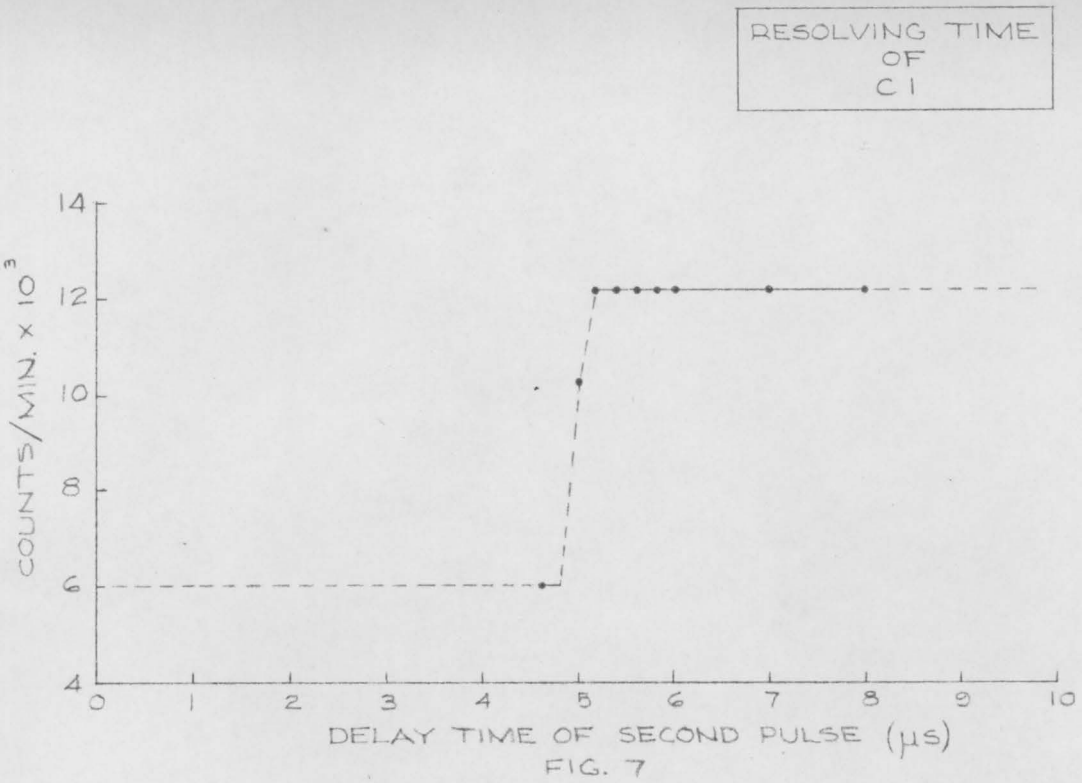
RESOLVING TIME
OF
C 1
COUNTS/MIN. x 10³
14
12
10
8
6
4
0
1
2
3
4
5
6
7
8
9
10
DELAY TIME OF SECOND PULSE (μs)

FIG. 7

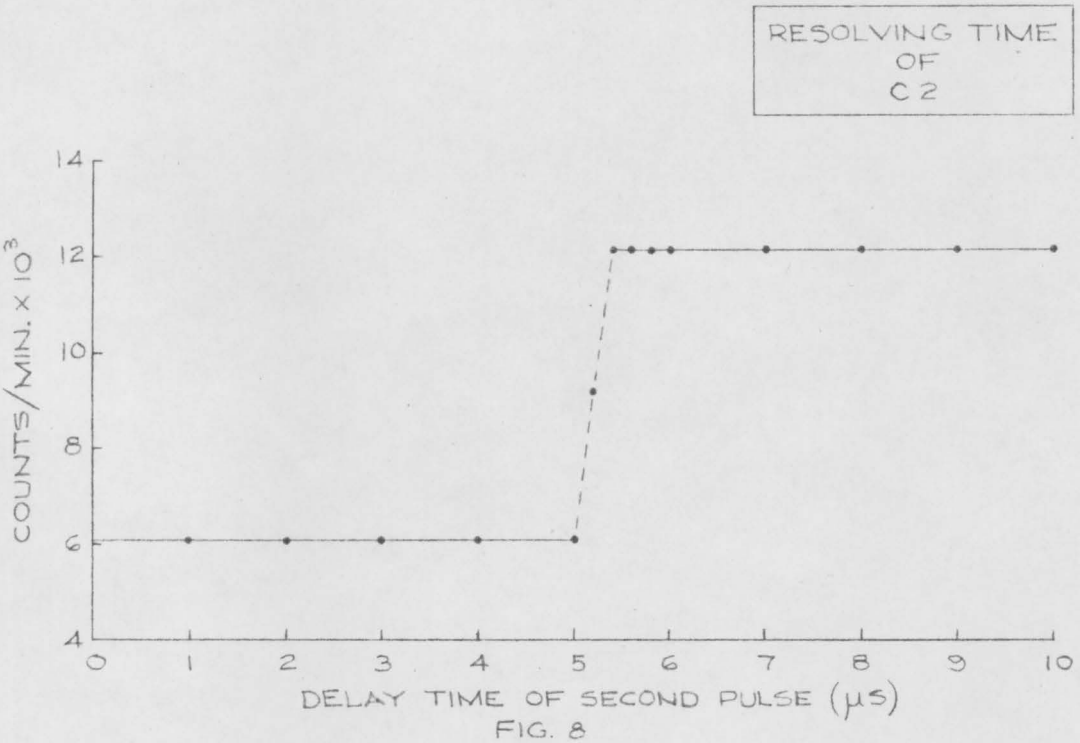
RESOLVING TIME
OF
C 2
COUNTS/MIN. x 10³
14
12
10
8
6
4
0
1
2
3
4
5
6
7
8
9
10
DELAY TIME OF SECOND PULSE (μs)

FIG. 8

TABLE 1. NEUTRON DENSITY A(z) vs. (z) IN FERRIC NITRATE SOLUTIONS

	Concentrated	First Dilution	Second Dilution	Third Dilution
Position	A(z)	A(z)	A(z)	A(z)
2	23.072	26.650	28.296	32.021
3	19.228	21.913	23.644	26.742
4	13.441	15.231	16.659	19.199
5	8.246	9.442	10.003	11.797
6	4.469	5.311	5.445	6.471
7	2.805	3.203	3.314	3.881
8	1.535	1.732	1.778	2.048
9	0.761	0.862	0.908	1.043
10	0.395	0.437	0.447	0.522

TABLE 2. NEUTRON DENSITY A(z) vs. (z) IN THORIUM NITRATE SOLUTIONS

	Concentrated	First Dilution	Second Dilution	Water
Position	A(z)	A(z)	A(z)	A(z)
2	20.101	23.034	27.858	31.599
3	16.431	18.466	23.518	26.721
4	11.652	13.308	16.604	19.431
5	7.235	8.180	10.284	11.830
6	3.988	4.501	5.489	6.588
7	2.359	2.617	3.220	3.892
8	1.293	1.410	1.738	2.109
9	0.658	0.722	0.884	1.062
10	0.319	0.357	0.439	0.515

VIII. DATA ANALYSIS

Cadmium ratios which varied from 40-80 and cadmium differences of 150-250 indicated that the bare detector was counting mostly neutrons with energy $E \leq 0.5$ ev (cadmium cut-off). The techniques of cadmium ratios and cadmium differences are standard techniques and are discussed in most texts (12). These techniques are based on the fact that the cross-section of cadmium in the low energy region looks somewhat like a step function, starting about 2400 barns in the thermal range, and rising to a peak of about 7200 barns at 0.18 ev. Therefore, the assumption is made that, for sufficiently thick cadmium, essentially all neutrons with energies less than some effective cut-off energy are absorbed in the cadmium shield. One is then able to tell approximately what the contribution to the total counting rate is due to neutrons of energies above and below this effective cut-off energy by taking the difference in counting rate with and without the cadmium shield ("cadmium difference"). Since the transmission of neutrons through cadmium is exponential in nature, the effective cut-off energy will vary slightly with cadmium thickness. The cut-off for 10 mil cadmium is approximately 0.4 ev, while it is between 0.5 and 0.6 ev for 30 mil thicknesses. In this experiment, the cadmium shield was approximately 30 mil thick. The cadmium ratio, R_{cd}, is defined as the ratio of the counting rate of the bare detector to the counting rate of the cadmium covered detector. (Many bare detectors normally used in measuring neutron

density or flux are sensitive to some extent to both thermal and resonance neutrons; when shielded with sufficient cadmium, they count essentially only resonance neutrons.) This ratio, R_{cd}, is expressed as

$$R_{cd} = \frac{\text{thermal counting rate + resonance counting rate}}{\text{resonance counting rate}} .$$

It is shown in Appendix A that, for an infinite system,

$$q_{Th}(u_t) = q(u_o)\, P_{Th}, \quad \text{and}$$

$$q_{Fe}(u_t) = q(u_o)\, P_{Fe} ,$$

where $q(u_t)$ = the slowing down density at lethargy u_t;

$q(u_o)$ = $q(0)$ = the slowing down density at source energy

P_{Th} = non-absorption probability for thorium

P_{Fe} = non-absorption probability for iron .

For a finite system, however, neutrons are lost by absorption and by leakage. Therefore, we have in a finite system,

$$q_{Th}(u_t) = q(u_o)\, P_{Th}\, P_{\alpha} , \text{ and}$$

$$q_{Fe}(u_t) = q(u_o)\, P_{Fe}\, P_{\alpha} ,$$

where P_{α} = non-leakage probability. Examination of the curves of neutron density versus spatial position for corresponding number densities (both total counts with bare detector, and fast counts with cadmium covered detector) shows that the spatial distribution of neutrons is essentially constant, indicating a constant leakage rate

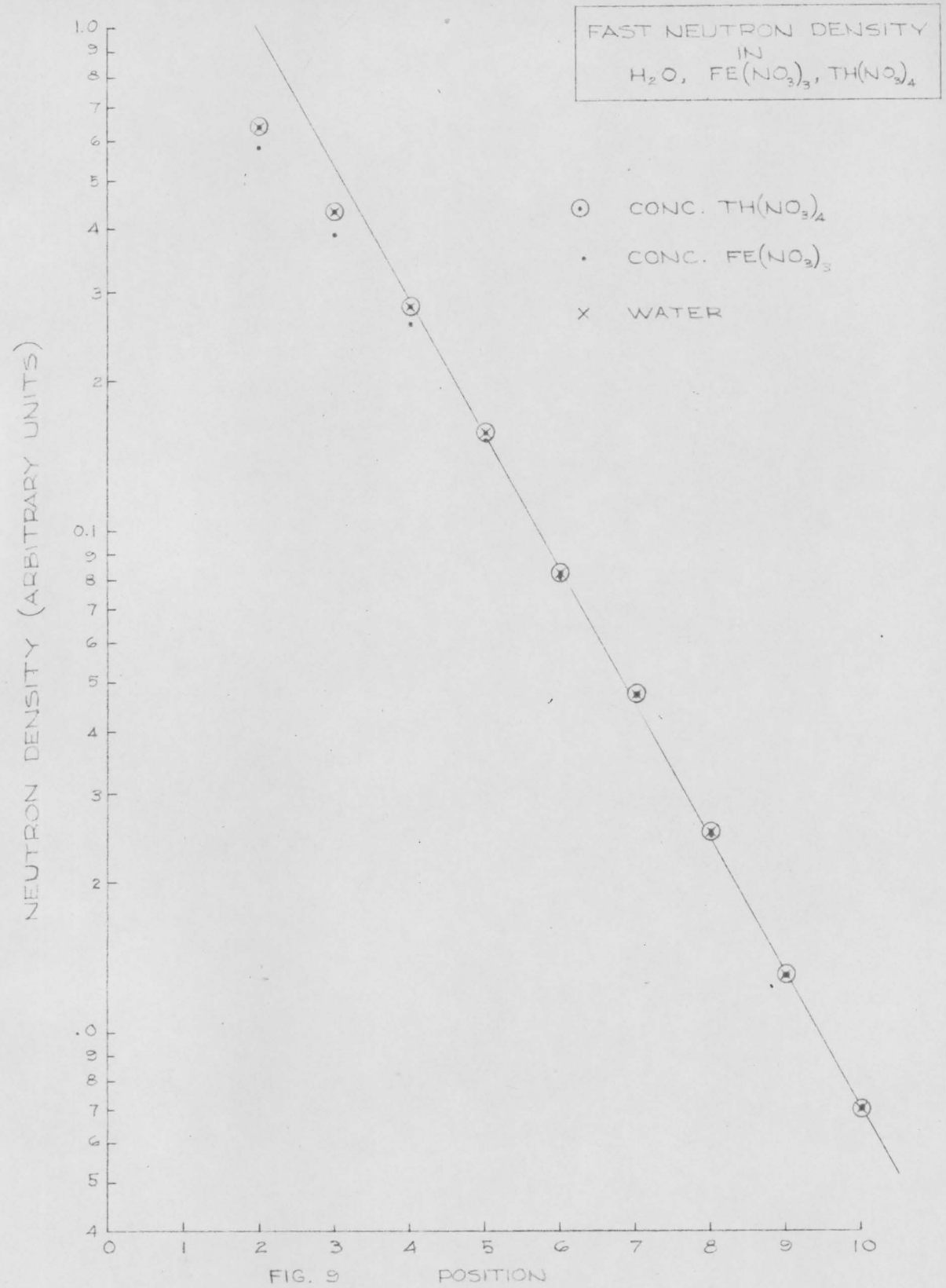
FAST NEUTRON DENSITY
IN
H_2O, $FE(NO_3)_3$, $TH(NO_3)_4$
⊙ CONC. $TH(NO_3)_4$
· CONC. $FE(NO_3)_3$
× WATER
NEUTRON DENSITY (ARBITRARY UNITS)
1.0
0.1
.0
0 1 2 3 4 5 6 7 8 9 10
POSITION

FIG. 9

for corresponding systems. This fact then allows us to cancel the non-leakage probabilities in the above equation. It is suggested, however, that if this method of determining R.E.P. is used over a wider range of concentrations or in more concentrated solutions, a measurement be made of leakage from the system and proper corrections applied.

Still using the previous notation, we have

$$q_{Th}(u_t) = \frac{q_{Fe}(u_t)}{P_{Fe}\,P_{\varepsilon}}\,P_{Th(nr)} \cdot P_{Th(r)} \cdot P_{\varepsilon} \cdot$$

We will now take the ratio $\frac{P_{Fe}}{P_{Th(nr)}}$ and define $k = \frac{P_{Fe}}{P_{Th(nr)}}$. Since $P_{Fe} = k\,P_{Th(nr)}$, we may write

$$q_{Th}(u_t) = \frac{q_{Fe}(u_t)}{k}\,P_{Th(r)},$$

or

$$P_{Th(r)} = \frac{k\,q_{Th}(u_t)}{q_{Fe}(u_t)},$$

which is the measured R.E.P., and which is also the R.E.P. for an infinite system, due to the cancellation of non-leakage probabilities of corresponding number densities of thorium and iron.

A. Discussion of Results

A comparison of experimental results for R.E.P.'$_\infty$* with Monte Carlo predictions (see Fig. 12) shows good correlation between the two. The greatest experimental errors lie in the determination of the neutron density. The efficiency of the counting systems was

*R.E.P.'$_\infty$ is the resonance escape probability for an infinite system, including neutrons which "skip" by the resonance region in one collision.

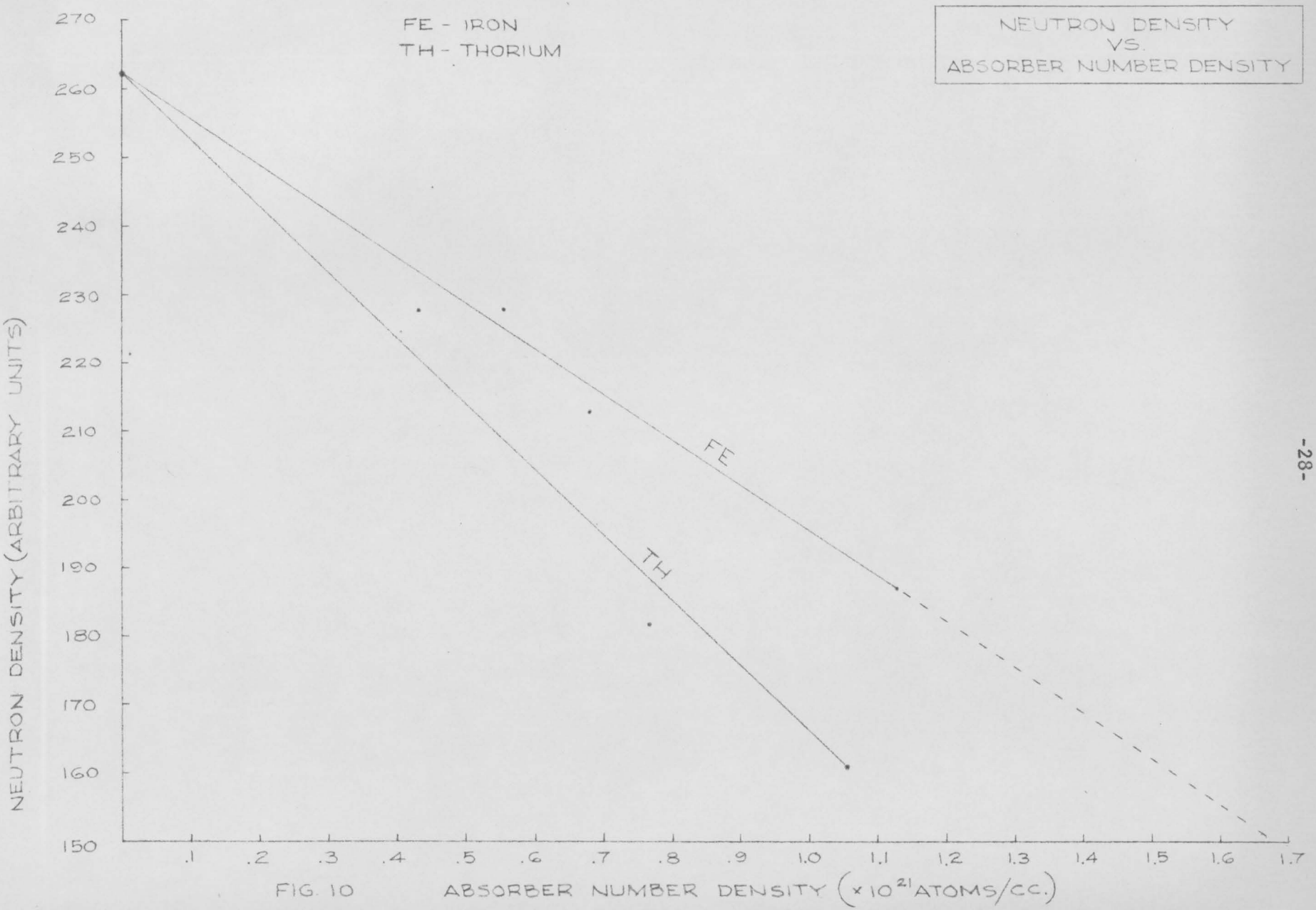
FE - IRON
TH - THORIUM
NEUTRON DENSITY
VS.
ABSORBER NUMBER DENSITY
NEUTRON DENSITY (ARBITRARY UNITS)
270
260
250
240
230
220
210
200
190
180
170
160
150
FE
TH
.1
.2
.3
.4
.5
.6
.7
.8
.9
1.0
1.1
1.2
1.3
1.4
1.5
1.6
1.7
ABSORBER NUMBER DENSITY (×10^21 ATOMS/CC.)

FIG. 10

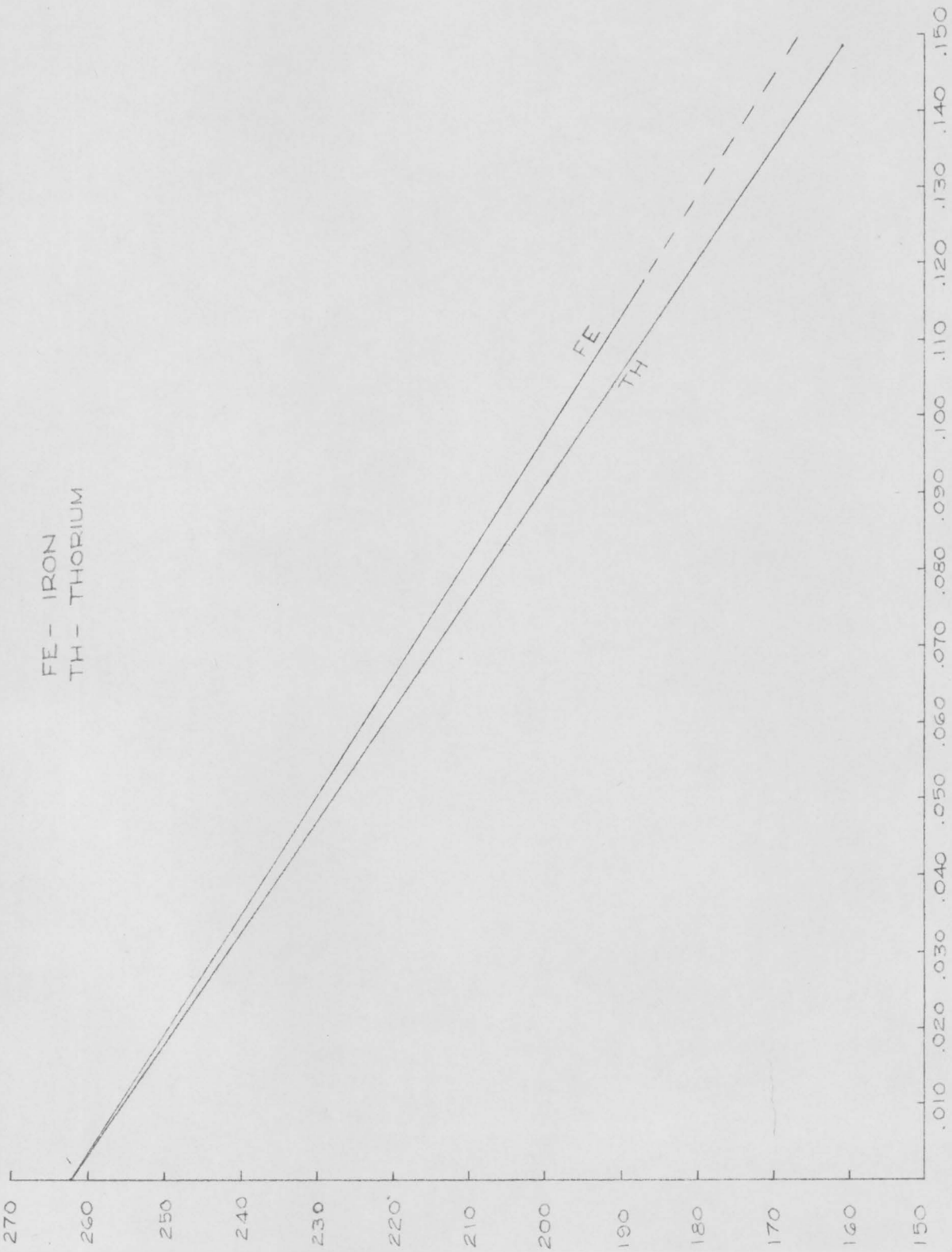
FE - IRON
TH - THORIUM
FE
TH
NEUTRON DENSITY (ARBITRARY UNITS)
270
260
250
240
230
220
210
200
190
180
170
160
150
.010 .020 .030 .040 .050 .060 .070 .080 .090 .100 .110 .120 .130 .140 .150
$N_{TH}\left(\frac{\sigma_a}{\sigma_s}\right)_{TH}$ ($\times 10^{21}$ ATOMS/CC)

FIG. 11

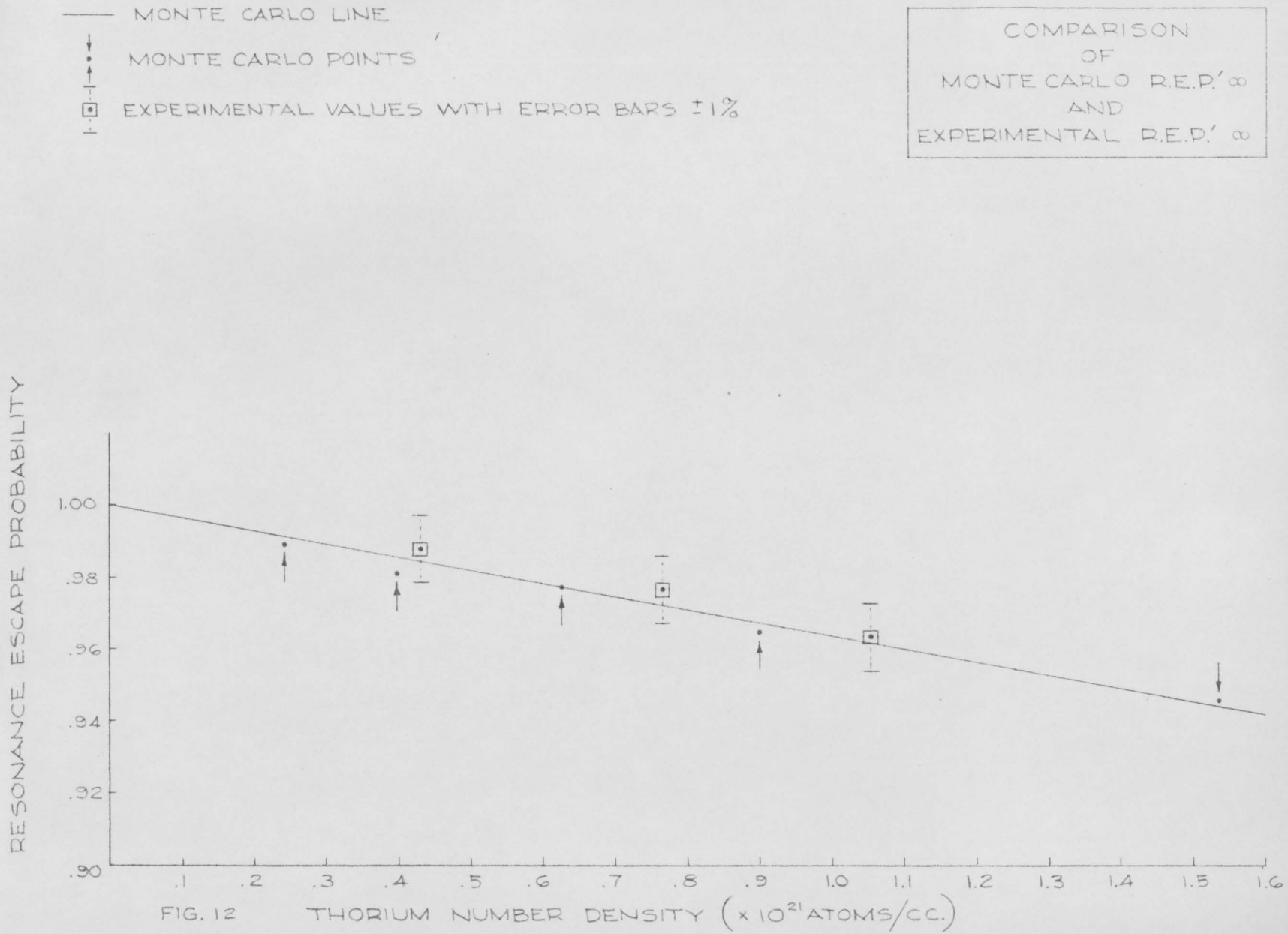
MONTE CARLO LINE
MONTE CARLO POINTS
EXPERIMENTAL VALUES WITH ERROR BARS ±1%
COMPARISON OF MONTE CARLO R.E.P.'∞ AND EXPERIMENTAL R.E.P.' ∞
RESONANCE ESCAPE PROBABILITY
1.00
.98
.96
.94
.92
.90
.1
.2
.3
.4
.5
.6
.7
.8
.9
1.0
1.1
1.2
1.3
1.4
1.5
1.6
THORIUM NUMBER DENSITY (× 10^21 ATOMS/CC.)

FIG. 12

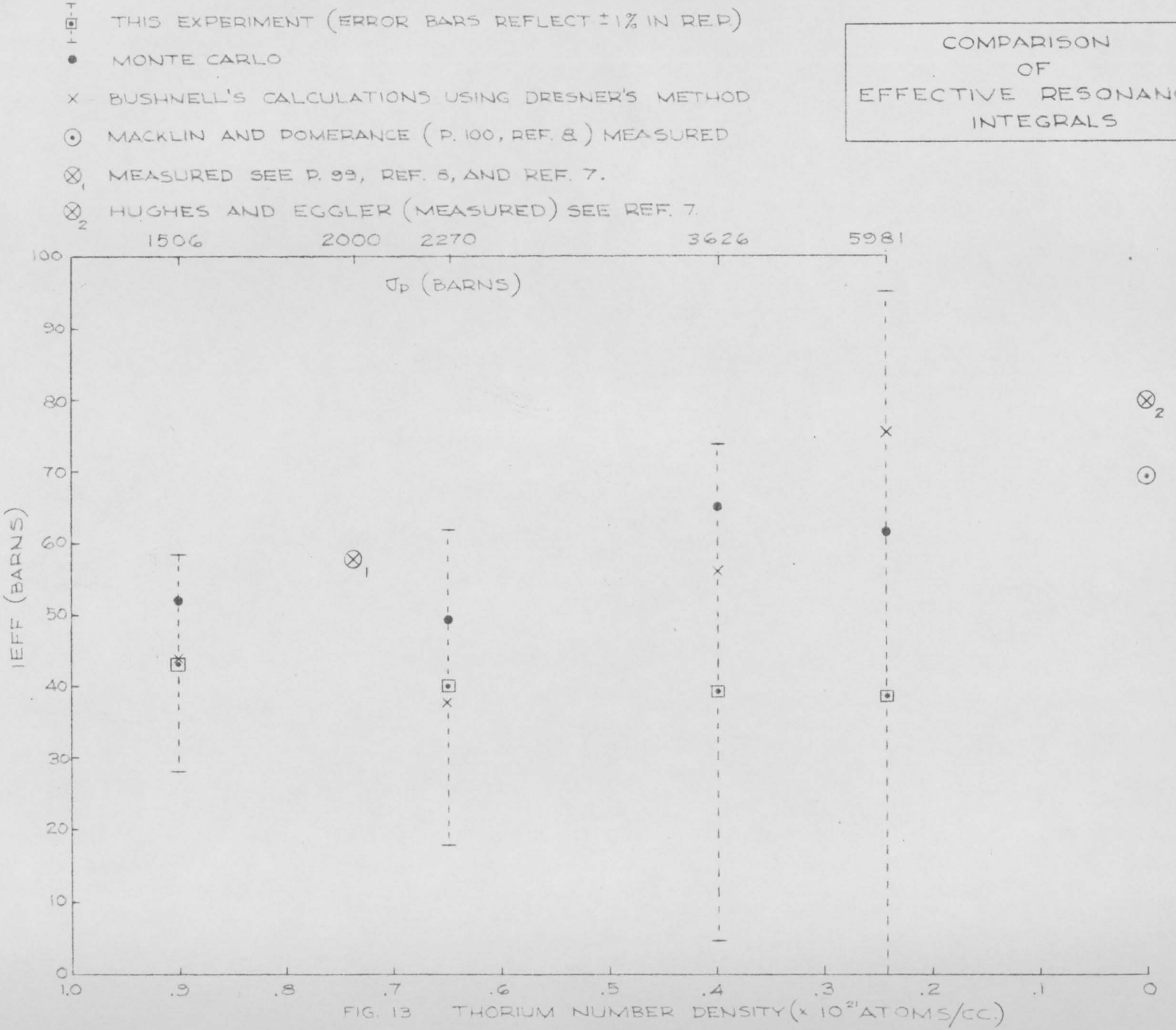
THIS EXPERIMENT (ERROR BARS REFLECT ± 1% IN REP)
MONTE CARLO
BUSHNELL'S CALCULATIONS USING DRESNER'S METHOD
MACKLIN AND POMERANCE (P. 100, REF. 8) MEASURED
MEASURED SEE P. 99, REF. 8, AND REF. 7.
HUGHES AND EGGLER (MEASURED) SEE REF. 7.
COMPARISON OF EFFECTIVE RESONANCE INTEGRALS
1506
2000
2270
3626
5981
σ_p (BARNS)
IEFF (BARNS)
100
90
80
70
60
50
40
30
20
10
0
1.0
.9
.8
.7
.6
.5
.4
.3
.2
.1
0
THORIUM NUMBER DENSITY (× 10^{21} ATOMS/CC.)

FIG. 13

examined periodically in standard geometry, and showed that measurements of neutron density are reliable to within two percent. Seven such checks show a maximum deviation of initial and "check" counts of 1.33 percent, a minimum of eight parts in thirteen thousand, and an average of 0.69 percent. Since the statistics on the measurements of neutron density are better (of the order of 10^6 counts) than those on the "checks" (10^5 - 10^6 counts), an assignment of $\pm$ 1 percent to these measurements is reasonable. It should be kept in mind that by utilizing the area under a curve of neutron density vs. position, minor fluctuations would tend to cancel out, while any significant long-term drifts in either direction would be noted in the routine checks.

The error in R.E.P. caused by reasonable changes in cross-sections used in computations is also small, and would lead to changes in values obtained for the R.E.P. of $\leq$ 3 percent.

In order to increase the reliability of neutron density comparisons between thorium and the equivalent iron concentrations, the lines of neutron density versus number density of absorber (Fig. 8) are drawn from the least concentrated solutions to the most concentrated solutions, thereby tending to minimize any possible discrepancies in the dilution and/or sampling procedures. It should be noted, however, that a least squares fit (which is considered less accurate in this case), would change the slope of both lines by approximately the same amount.

Even though this experiment is designed to measure the R.E.P. rather than the effective resonance integral (I_{eff}), a comparison of I_{eff} calculated from both the experimental and Monte Carlo values of R.E.P. is made in Fig. 13. Two things should be noted in the interpretation of this graph. First, it should be noted, as mentioned above, that determining I_{eff} from the R.E.P. is not normally done, since an uncertainty of 1 percent in the R.E.P. may cause an uncertainty of order of 100 percent in I_{eff}. Second, the values obtained for I_{eff} from Monte Carlo values of R.E.P. and the values of R.E.P. obtained from this experiment are for absorption in the resonance region. The I_{eff} normally reported is composed of this quantity ($I_{eff(res)}$) plus the small contribution between cadmium cut-off and the resonance region, and the small contribution above the resonance region. Therefore, a correction (2.5 barns) has been added to our $I_{eff(res)}$ to yield a value of $I_{eff(total)}$ which is directly comparable with other experimental determinations of I_{eff}.

B. Summary

An experiment was performed on aqueous solutions of thorium nitrate and ferric nitrate to determine the resonance escape probability of thorium in such a system with physical dimensions of 61 cm. x 61 cm. x 33 cm. Neutrons for the experiment were obtained by the D(d, n) He^3 reaction with deuterons from a Cockcroft-Walton 200 kev accelerator. The neutron density was examined at given spatial points as a function of concentration of the above salts. By

compensation for spectral changes of the neutrons in the energy range "seen" by the bare detector, it was possible to subtract the absorption due to a smooth thorium cross-section from the actual cross-section, thereby giving the effect of absorption in the resonance peaks. The correlation with the Monte Carlo calculations in the range of the experiment is good, being within 1 percent.

IX. ACKNOWLEDGEMENTS

The author is indebted to many people for their aid in this experiment and in his graduate studies:

To the United States Atomic Energy Commission for financial support of the experiment,

To the members of his graduate committee; Dr. James A. Jacobs, Department Head; Dr. Andrew Robeson, thesis advisor; Dr. A. Keith Furr; Dr. Clarence D. Bond, and Dr. Svend T. Gormsen, for their advice and review of the thesis,

To Dr. W. G. Pettus of Babcock and Wilcox for his critical review of the rough thesis,

To all the graduate students who have contributed to the construction and/or experiment; to , co-worker;

, , ,

, and ,

To for her typing of the smooth thesis, and

for his drawing,

And mostly to his wife, for her sacrifices and encouragement during the years of graduate school.

X. BIBLIOGRAPHY

1. David L. Bushnell, A Monte Carlo Calculation of the Resonance Escape Probability of Thorium in a Homogeneous Reactor. Ph.D. Thesis, VPI, 1961.

2. E. Creutz, H. Jupnik, T. Snyder, and E. P. Wigner, Review of the Measurements of the Resonance Absorption of Neutrons by Uranium in Bulk. Journal of Applied Physics 26, p. 257, 1955.

3. E. P. Wigner, E. Creutz, H. Jupnik, and T. Snyder, Resonance Absorption of Neutrons by Spheres. Journal of Applied Physics 26, p. 260, 1955.

4. E. Creutz, H. Jupnik, T. Snyder, and E. P. Wigner, Effect of Geometry on Resonance Absorption of Neutrons by Uranium. Journal of Applied Physics 26, p. 271, 1955.

5. Allan C. G. Mitchell, Leon J. Brown, John R. Pruett, and Evar D. Nering, Resonance Absorption of Uranium in Mixtures. CP-1676, 1944.

6. N. Goldstein and D. J. Hughes, Resonance Absorption of Uranium. CP-3580, 1946.

7. D. J. Hughes and C. Eggler, Resonance Absorption of Thorium. CP-3093, 1945.

8. R. L. Macklin and H. S. Pomerance, Resonance Capture Integrals. Proceedings of the International Conference on the Peaceful Uses of Atomic Energy 5, p. 96, 1956.

9. P. E. Spivak, B. G. Erozolimsky, V. I. Lavrenchik, and G. E. Dorofeyev, Measurements of the Resonance Absorption Integrals and ν_{eff}- the Multiplication Coefficient of Resonance Neutrons for Fissionable Isotopes. Proceedings of the International Conference on the Peaceful Uses of Atomic Energy 5, p. 91, 1956.

10. Lawrence Dresner, Resonance Absorption in Nuclear Reactors. Pergamon Press, 1960.

11. Robert V. Meghreblian and David K. Holmes, Reactor Analysis. McGraw-Hill Book Co., 1960.

12. D. J. Hughes, Pile Neutron Research. Addison-Wesley Publ. Co., 1953.

13. Samuel Glasstone and Milton C. Edlund, The Elements of Nuclear Reactor Theory, D. Van Nostrand Co., 1952.

14. Alvin M. Weinberg and Eugene P. Wigner, The Physical Theory of Neutron Chain Reactors, The University of Chicago Press, 1958.

15. William J. Price, Nuclear Radiation Detection. McGraw-Hill Book Co., 1958.

16. Nordheim, L. W., GAMD-638, 1959.

17. Nordheim, L. W. and Samson, J. B., Trans. Amer. Nucl. Soc. 2, No. 1, Abstract 11-5, June 1959.

The vita has been removed from the scanned document

APPENDIX A. DERIVATION OF STANDARD EXPRESSION FOR RESONANCE ESCAPE PROBABILITY

An application of the laws of conservation of linear momentum and energy to perfectly elastic neutron collisions with nuclei initially at rest shows that the kinetic energy (E) of a neutron in the laboratory after collision is related to its initial kinetic energy (E_o) by

$$E = \frac{E_o}{(A+1)^2}(A^2 + 2\eta A + 1)$$

where $A = \frac{M}{m}$

M = mass of nucleus

m = mass of neutron

$\eta = \cos\beta$

β = angle between the initial and final velocities of the neutron in the center of mass system.

The maximum value of E is seen to be E_o, while the minimum value is

$$E_{min} = \frac{E_o}{(A+1)^2}(A^2 - 2\eta A + 1) = E_o \frac{(A-1)^2}{(A+1)^2} = \alpha E_o \quad ,$$

where $$\alpha = \left(\frac{A-1}{A+1}\right)^2 \quad .$$

We may now define a frequency function, f, which describes the angular distribution of neutrons emerging from a collision between a neutron of given speed and a nucleus of a particular type:

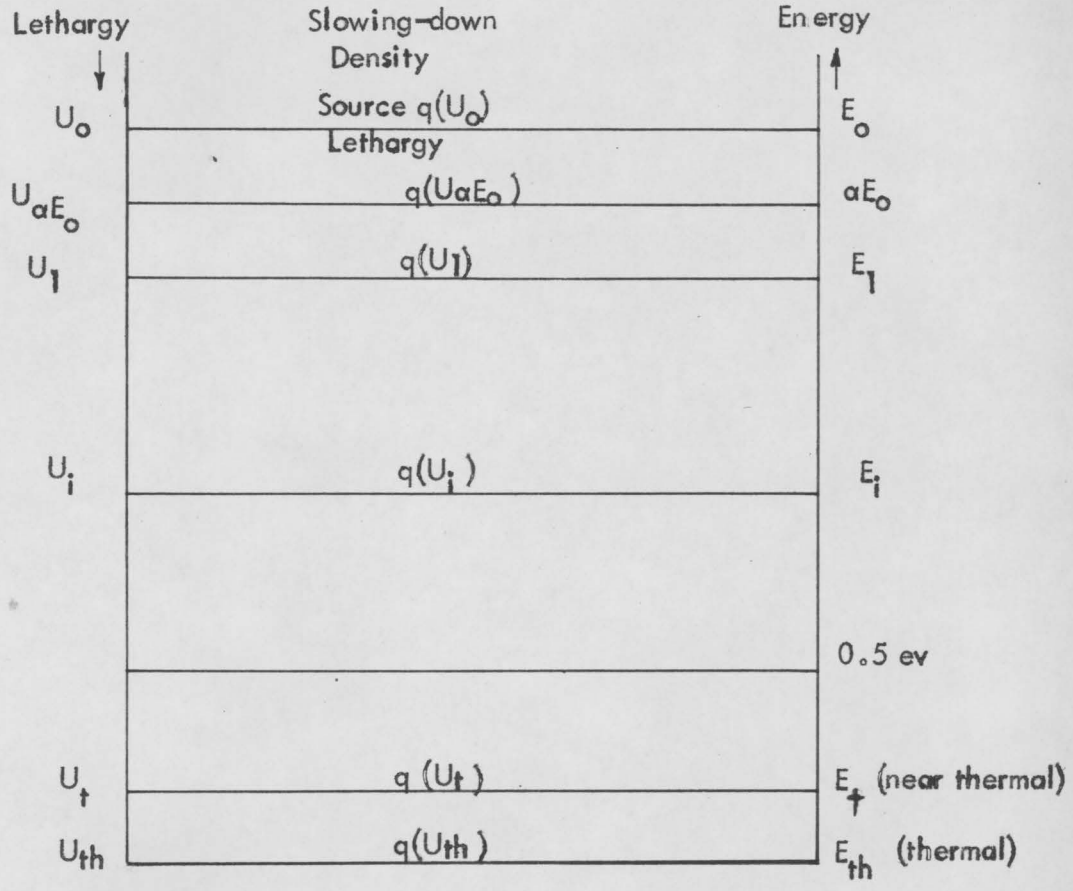

Figure 14

Energy, Lethargy and Slowing-down Density Relationships

$f(\eta)d\eta$ = fraction of all scattering collisions which result in scattering angles in the C.M. system whose cosines lie between η and $\eta + d\eta$.

For isotropic scattering in the center-of-mass system, the cosine of the scattering angle η is uniformly distributed between - 1 and 1. $f(\eta)$ is therefore a constant and its value is 1/2. We next define a frequency function in energy by

$h(E,E_o)dE$ = fraction of all scattering collisions which result in final kinetic energies of neutrons in range E to E + dE, where $\alpha E_o \leq E \leq E_o$.

We require that the probability that a certain event occur be the same regardless of the independent variable (E or η) used to describe it. This implies

$$h(E,E_o)dE = f(\eta)d\eta \quad .$$

h, f, hdE and f $d\eta$ are positive quantities; therefore,

$$h(E,E_o) = f(\eta)\frac{d\eta}{dE} \quad .$$

From $$E = \frac{E_o}{(A+1)^2}(A^2 + 2\eta A + 1)$$

we find $$\frac{d\eta}{dE} = \frac{(A+1)^2}{2AE_o} \quad .$$

Therefore

$$h(E,E_o) = \frac{1}{2} \cdot \frac{(A+1)^2}{2AE_o} = \frac{(A+1)^2}{4AE_o} = \frac{1}{(1-\alpha)E_o} \quad .$$

We may transform this energy frequency function to one in lethargy. The lethargy, u, of a neutron of kinetic energy E, is defined as

$$u = \ln \frac{E_{ref}}{E}$$

where E_{ref} is the highest energy of interest.

The frequency function (g) in lethargy space is defined as:

$g(u,u_o)\,du$ = probability that a neutron of lethargy u_o when scattered emerges with a lethargy between u and u + du

We require that

$$\left| g(u,u_o)\,du \right| = \left| h(E,E_o)\,dE \right|$$

and

$$g(u,u_o) = h(E,E_o)\left|\frac{dE}{du}\right| .$$

From the definition of lethargy

$$u = \ln \frac{E_{ref}}{E}$$

we have

$$du = -\frac{dE}{E} , \quad \text{and} \quad \frac{dE}{du} = -E .$$

Now

$$e^{u} = e^{\ln \frac{E_{ref}}{E}} \quad \text{and} \quad e^{-u} = e^{-\ln \frac{E_{ref}}{E}}$$

$$e^{(u_o-u)} = e^{\ln \frac{E_{ref}}{E_o} - \ln \frac{E_{ref}}{E}} = e^{\ln \frac{\frac{E_{ref}}{E_o}}{\frac{E_{ref}}{E}}} = \frac{E}{E_o}$$

$$g(u,u_o) = \frac{1}{(1-\alpha)\,E_o} \left| -E \right| = \frac{E}{E_o}\left(\frac{1}{1-\alpha}\right) = \frac{e^{-(u-u_o)}}{1-\alpha} .$$

The corresponding distribution function, $G(u,u_o)$ is defined to be

$$G(u,u_o) = \int_{u_o}^{u} g(u',u_o)\, du' \qquad \text{(where prime here denotes variable of integration)}$$

$$= \int_{u_o}^{u} \frac{e^{-u'} \cdot e^{u_o}}{1-\alpha}\, du' = \frac{e^{u_o} - e^{-u} + e^{-u_o}}{1-\alpha} = \frac{1 - e^{-(u-u_o)}}{1-\alpha} .$$

This is the probability that a neutron with an initial lethargy u_o emerges with lethargy $\leq u$. The probability of a neutron of lethargy u_o emerging from the scattering process with lethargy $> u$ is

$$1 - G(u,u_o) = 1 - \frac{1 - e^{-(u-u_o)}}{1-\alpha} = \frac{1 - \alpha - 1 + e^{-(u-u_o)}}{1-\alpha} = \frac{e^{-(u-u_o)} - \alpha}{1-\alpha}$$

The total number of neutrons scattered from du' which emerge with lethargy greater than u is then

$$\Sigma_s(u')\, \phi(u') \left[\frac{e^{-(u-u')} - \alpha}{1-\alpha}\right] du' .$$

The "slowing-down density", q(u) is defined as the number of neutrons crossing lethargy u per second per unit volume. In order to obtain the total contribution to the slowing-down density q(u) from all intervals du', we integrate the above from lethargy u_o corresponding to E_o to lethargy u, corresponding to E. To eliminate the necessity for a correction for the first-flight losses, we modify the limits and specify the minimum lethargy. As was indicated previously (p.40,41) the energy range of interest is from $\frac{E}{\alpha}$ to E where $\frac{E}{\alpha} < E_o$. The corresponding lethargy interval becomes u to $u - \ln \frac{1}{\alpha}$ where

$u > u_o + \ln \frac{1}{\alpha}$. Thus, the slowing-down density becomes:

$$q(u) = \int_{u-\ln\frac{1}{\alpha}}^{u} \Sigma_s (u')\, \phi(u') \left[\frac{e^{-(u-u')} - \alpha}{1 - \alpha}\right] du' \,.$$

$$u > u_o + \ln \frac{1}{\alpha}$$

Choosing the reference energy E_{ref} as E_o implies that $u_o = 0$.

We now consider the above equation for q(u) and introduce the condition that

$$\frac{d}{du}\, q(u) = - \Sigma_a (u)\, \phi(u)$$

where $q(u_o)$ is defined as q_o.

For small absorption, $\phi(u)$ is a slowly varying function, and $\Sigma_s (u')\, \phi(u')$ can be expanded in a Taylor series about u. Retaining the first two terms, we have

$$\Sigma_s (u')\, \phi(u') \approx \Sigma_s(u)\, \phi(u) + (u' - u) \frac{d}{du}\left[\Sigma_s(u)\, \phi(u)\right] \,.$$

Substituting this in the equation for q(u):

$$q(u) = \frac{1}{1 - \alpha} \int_{u-\ln\frac{1}{\alpha}}^{u} \left\{ \Sigma_s(u)\, \phi(u) + (u' - u) \frac{d}{du} \Sigma_s(u)\, \phi(u) \right\} \cdot \left[e^{(u'-u)} - \alpha\right] du' \,.$$

If we define

$$\gamma = 1 - \frac{\alpha \ln^2 \alpha}{2\xi\ (1 - \alpha)}$$

and define $\xi = \overline{\ln \frac{E_o}{E}} = \int_{\alpha E_o}^{E_o} \ln \frac{E_o}{E}\ h(E,E_o)\ dE$

$$= \int_{\alpha E_o}^{E_o} \ln \left(\frac{E_o}{E} \right) \frac{dE}{(1 - \alpha)\ E_o} = 1 + \frac{\alpha \ln \alpha}{1 - \alpha} \ ,$$

q(u) becomes upon integration

$$q(u) \approx \xi \sum_s (u)\ \phi(u) - \gamma\xi \frac{d}{du} \left[\sum_s (u)\ \phi(u) \right] \ .$$

As a first approximation, we take

$$q(u) \approx \xi \sum_s (u)\ \phi(u)\ \frac{d}{du}\ q(u) = \xi \frac{d}{du} \left[\sum_s (u)\ \phi(u) \right] \ .$$

If this approximate derivative is substituted in the above result of integration, we have

$$q(u) \approx \xi \sum_s (u)\ \phi(u) - \gamma\xi \cdot \frac{1}{\xi} \frac{d}{du}\ q(u) \ .$$

If we refer to our previous assumption that

$$\frac{d}{du}\ q(u) = - \sum_s (u)\ \phi(u)$$

and use this relationship for q(u)

$$q(u) \approx \xi \sum_s (u)\ \phi(u) - \gamma \left[- \sum_s (u)\ \phi(u) \right]$$

$$q(u) \approx \left[\xi \sum_s (u) + \gamma \sum_a (u) \right] \phi(u) \quad .$$

But $\phi(u)$ from the above assumption is

$$\phi(u) = - \frac{1}{\sum_a (u)} \frac{d}{du} q(u) \quad .$$

So
$$q(u) \approx - \left[\xi \sum_s (u) + \gamma \sum_a (u) \right] \frac{1}{\sum_a (u)} \frac{dq(u)}{du} \quad .$$

or
$$\frac{dq(u)}{du} + \frac{\sum_a (u)}{\xi \sum_s (u) + \gamma \sum_a (u)} q(u) = 0 \quad .$$

This is a linear differential equation whose integrating factor is

$$I = \exp \left[\int_o^u \frac{\sum_a (u)}{\xi \sum_s (u) + \gamma \sum_a (u)} du \right] .$$

The solution is

$$qI = \text{constant (C)} \quad .$$

$$q(u) \exp \left[\int_o^u \frac{\sum_a (u)}{\xi \sum_s (u) + \gamma \sum_a (u)} du \right] = C \quad .$$

$$q(u) = C \exp \left[- \int_o^u \frac{\sum_a (u)}{\xi \sum_s (u) + \gamma \sum_a (u)} du \right] .$$

$$q(u) = q_o \exp \left[- \int_o^u \frac{\sum_a (u)}{\xi \sum_s (u) + \gamma \sum_a (u)} du \right] .$$

The nonabsorption probability for a system containing some absorbing material is given by the above exponential. In general for any

interval u_1 to u_2, the nonabsorption probability, or resonance escape probability, is defined by

$$\text{R.E.P.} = \exp - \int_{u_1}^{u_2} \frac{\sum_a (u)}{\xi \sum_t (u)} \, du$$

if the assumption is made that $\xi \approx \gamma$.

Using the above notation, the probability of a neutron going from source lethargy to the lethargy corresponding to E_t, where E_t is an undefined mean energy of the measured neutron population in the system, is P. This energy will be near thermal, and < 0.5 ev, but need not be known precisely in this case.

For iron, we may write

$$q_{Fe}(u_t) = q(u_o) P_{Fe} ,$$

where $q_{Fe}(u_t)$ is the slowing down density at u_t, the lethargy corresponding to E_t, the energy somewhere near "thermal", $q(u_o)$ is the slowing down density at source lethargy, and P_{Fe} is the non-absorption probability of a neutron traversing the lethargy range from u_o to u_t in the ferric nitrate solution.

We may write an analogous equation for thorium:

$$q_{Th}(u_t) = q(u_o) P_{Th} ,$$

where P_{Th} is the non-absorption probability for a neutron traversing the same lethargy range in the thorium nitrate solution, and is composed of the non-resonance non-absorption probability ($P_{Th(nr)}$) and resonance non-absorption probability ($P_{Th(r)}$). The non-resonance absorption is the absorption which would be exhibited by thorium if

it had a smooth cross-section without resonances. Thus,

$$P_{Th} = P_{Th(nr)} \cdot P_{Th(r)} \ ,$$

where the subscripts r and nr refer to resonance and non-resonance conditions respectively, and the above is true since $P_{Th(nr)}$ and $P_{Th(r)}$ as defined are independent probabilities.

Noting that $P_{Fe} = kP_{Th(nr)}$, we may solve for $q(u_o)$ from the iron equation and substitute in the thorium equation:

$$q(u_o) = \frac{q_{Fe}(u_t)}{P_{Fe}}$$

$$q_{Th(u_t)} = \left(\frac{q_{Fe}(u_t)}{P_{Fe}} \right) \cdot P_{Th}$$

$$= \left(\frac{q_{Fe}(u_t)}{P_{Fe}} \right) \left(P_{Th(nr)} \cdot P_{Th(r)} \right)$$

$$= \left(\frac{q_{Fe}(u_t)}{k} \right) \cdot P_{Th(r)}$$

or

$$P_{Th(r)} = \frac{k q_{Th}(u_t)}{q_{Fe}(u_t)} \ .$$

k, the ratio of $\frac{P_{Fe}}{P_{Th}}$, is evaluated by comparing the probability of non-absorption of a neutron upon interaction with equal number densities of absorbers. The probability of non-absorption per interaction is given by $P = \frac{\sigma_s}{\sigma_t}$. A calculation of p for $Fe(NO_3)_3$ and for $Th(NO_3)_4$ shows k is, within the accuracy of the cross-sections, equal to 1.0.

It is shown (Ref. 13, p. 160, 171) that in the asymptotic case, when the neutron energies are less than αE_o, that $q = \bar{\xi} \sum_s \phi(u)$ for a weakly absorbing system.

Also, it is seen that the reaction rate in a detector containing B^{10} is a function of ϕ. (Ref. 15, p. 260) The contribution dR to the reaction rate by neutrons between the energy E and E + dE in the volume element dV is

$$dR = N(r)\ \sigma(E)\ \phi(E, r)\ dE dV$$

where $N(r)$ = number of B^{10} atoms per unit volume at point r.

$\sigma(E)$ = B^{10} (n,α) cross-section at energy E.

$\phi(E,r)$ = flux per unit energy interval at point r.

We may see then, that $dR \propto \phi \propto q$, and may write

$$P_{Th(r)} = \frac{kR_{Th}}{R_{Fe}}$$

where R_{Th} and R_{Fe} are the normalized counts at a given point, corrected to the same value of $F = \left(\frac{\sum_a}{\bar{\xi} \sum_s} \right)$, a procedure which compensates for the differences in the "Maxwellian" thermal flux in the thorium and iron systems. (See Appendix B.)

If, however, instead of the normalized counts at a point, we plot normalized counts versus (z), we have a more reliable measurement of $q_{Th}(u_t)$ and $q_{Fe}(u_t)$ for comparison. Therefore, we now write

$$P_{Th(r)} = \frac{A_{Th}}{A_{Fe}}$$

where A_{Th} and A_{Fe} represent the areas under curves of counts versus (z), properly normalized and corrected to the same value of F.

APPENDIX B. CORRELATION OF FLUX DISTRIBUTIONS

In order to properly compare the counting rates obtained with a BF_3 detector in solutions of the same absorber number densities, but which have different nuclear parameters, one must compensate for changes in the Maxwellian distribution of the neutrons in the thermal region. We will identify the following parameters:

E_o = the most probable energy of the Maxwellian distribution

E_1 = the energy at which the Maxwellian and 1/E fluxes join.

It is shown in standard texts that

(1) $q(E_1) = \phi_T \overline{\overline{\sum}}_a$, and that

(2) $\phi(E) = \dfrac{q_o P_r P_{nr}}{\bar{\xi} \sum_s E}$, where

$\phi(E)$ = flux at energy E

P_r = resonance escape probability

P_{nr} = non-resonance escape probability

$\bar{\xi}$ = average logarithmic energy decrement per collision

$\sum_s$ = macroscopic scattering cross-section

$q(E_1)$ = slowing down density at energy E_1

q_o = slowing down density at source energy

ϕ_T = total flux = $\int_o^\infty \phi(E)\, dE$

$\overline{\overline{\sum}}_a$ = macroscopic absorption cross-section corresponding to average energy

For a weakly absorbing system, we may write:

(3) $$\bar{\xi} \sum_s E_1 \phi(E_1) = \phi_T \overline{\overline{\sum}}_a$$

The Maxwellian flux is given by:

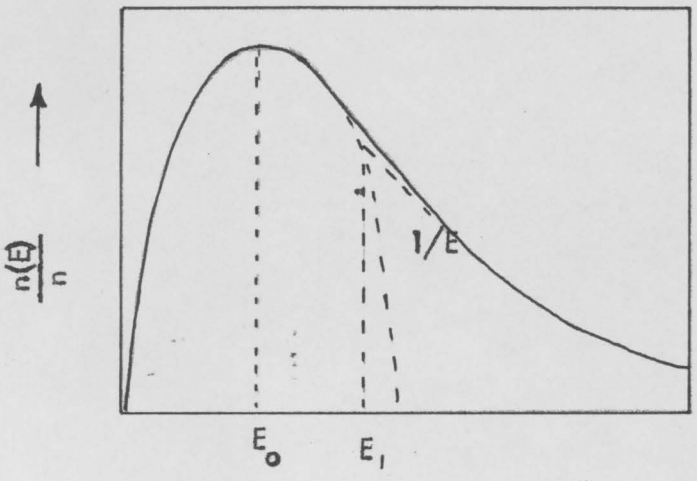

Fig. 15

MAXWELL-BOLTZMANN DISTRIBUTION OF ENERGY (ILLUSTRATING THE "MAXWELLIAN" AND "1/E" REGIONS)

E_o = most probable Maxwellian energy

E_1 = Junction between "Maxwellian" and "1/E" regions

$$(4) \qquad \phi_M(E) = \frac{\phi_T}{E_o^2} E \; e^{-E/E_o}$$

The Maxwellian flux at energy E_1 is then

$$(5) \qquad \phi_M(E_1) = \frac{\phi_T}{E_o^2} E_1 \; e^{-E_1/E_o}$$

But $\phi_M(E_1) = \frac{P_r \; P_{nr}}{\bar{\xi} \sum_s E_1}$ from (2) for a unit source.

So $$\frac{P_r \; P_{nr}}{\bar{\xi} \sum_s E_1} = \frac{\phi_T}{E_o^2} E_1 \; e^{-E_1/E_o}$$

If we invoke the boundary condition that $\phi_{1/E}(E_1) = \phi_M(E_1)$, and substitute for $\phi(E_1)$ in Eq. (3):

$$\bar{\xi} \sum_s E_1 \left(\frac{\phi_T}{E_o^2} E_1 \; e^{-E_1/E_o} \right) = \phi_T \bar{\Sigma}_a$$

we obtain

$$\frac{E_1^2}{E_o^2} e^{-E_1/E_o} = \frac{\bar{\Sigma}_a}{\bar{\xi} \sum_s}$$

which says that if two thermal distributions are the same, their values of $\frac{\bar{\Sigma}_a}{\bar{\xi} \sum_s}$ will be the same. Conversely, in order to compensate for changes in the flux distributions of two systems, we will require that equal values of $\frac{\bar{\Sigma}_a}{\bar{\xi} \sum_s}$ be compared, rather than equal number densities of absorbers.

The criterion for comparison of "thermal" counting rates in absorbing solutions being established as $\frac{\bar{\Sigma}_a}{\bar{\xi} \sum_s} = F$, we may compute F for ferric nitrate and thorium nitrate, noting that $\bar{\xi}$ is essentially

the same for comparable absorber number densities in these dilute hydrogeneous media:

$$F_{Abs} = \frac{N_{Abs}\ (\sigma_{a\ Abs}) + N_{NO_3}(\sigma_{a\ NO_3})}{N_{Abs}\ (\sigma_{s\ Abs}) + N_{NO_3}(\sigma_{s\ NO_3})}$$

where $F_{Abs} = F_{Th}$ or F_{Fe}

N_{Abs} = number of absorber atoms used in the comparison (= 1)

N_{NO_3} = number of nitrate radicals per absorber atom (3 or 4)

$\sigma_{NO_3} = \sigma_N + 3\ \sigma_o$

We thus obtain values for F_{Fe} and F_{Th} of 0.10368 and 0.1408 when $\xi = 1$. The change in variable in the plot of neutron density vs. absorber number density to neutron density vs. F is then accomplished by translation of points of one line in the first plot with respect to the other line as indicated by the ratio of F's. The measured neutron densities are thereby given as a function of F, and their ratios are taken for a given F value to determine the resonance escape probability, as shown in Appendix A.

APPENDIX C. TABULATIONS OF DATA AND VALUES OF PARAMETERS USED

TABLE 3. NEUTRON DENSITY A(z) vs. (z) POSITION IN CONCENTRATED FERRIC NITRATE

Position (cm.)	A(z) (arbitrary units)
0	0.678
0.6	0.876
1.6	1.014
2.6	1.066
3.6	1.035
4.6	0.974
5.6	0.885
6.6	0.784
7.6	0.696
8.6	0.603
9.6	0.518
10.6	0.439
11.6	0.376
12.6	0.290
13.6	0.260
14.6	0.212
15.6	0.178
16.6	0.164
17.6	0.129
18.6	0.107
19.6	0.086
20.6	0.072
21.6	0.059
22.6	0.048
23.6	0.040
24.6	0.037
25.6	0.026
26.6	0.022

TABLE 4. NEUTRON DENSITY vs. ABSORBER NUMBER DENSITY

Thorium Solution	Thorium Number Density ($\times 10^{21}$ atoms/cc.)	Neutron Density (arbitrary units)
Concentrated	1.054	161
First Dilution	0.768	182
Second Dilution	0.431	228
Water	0.000	262

Iron Solution	Iron Number Density ($\times 10^{21}$ atoms/cc.)	Neutron Density (arbitrary units)
Concentrated	1.128	187
First Dilution	0.680	213
Second Dilution	0.558	228
Third Dilution	0.000	262

TABLE 5. COMPARISON OF MONTE CARLO AND EXPERIMENTAL VALUES OF R.E.P. ∞

A	B	C	D	E	F
Thorium Number Density ($\times 10^{21}$ atoms/cc.)	Thorium Neutron Density	Corresponding Iron Neutron Density	Experimental R.E.P.(B/C)	Monte Carlo R.E.P. ∞	Percentage Difference
0.1000	252.4	253.1	0.997±0.01		
0.2000	242.8	244.1	0.995±0.01		
0.2439	238.6	240.2	0.993±0.01	0.9893	0.42
0.3000	233.2	235.2	0.992±0.01		
0.3991	223.6	226.1	0.989±0.01	0.9814	0.76
0.5000	214.0	217.1	0.986±0.01		
0.6000	204.5	208.1	0.983±0.01		
0.6231	202.3	206.0	0.982±0.01	0.9778	0.42
0.7000	194.9	199.1	0.979±0.01		
0.8000	185.3	190.0	0.975±0.01		
0.9000	175.7	181.0	0.971±0.01		
0.9013	175.6	183.2	0.971±0.01	0.9649	0.59
1.0000	166.05	172.05	0.965±0.01		

TABLE 6. VALUES OF I_{eff} FROM THEORY AND EXPERIMENT (See Fig. 13)

Thorium Number Density ($\times 10^{21}$ atoms/cc.)	Experimental I_{eff}* (barns) $I_{eff(res)}$	$I_{eff(total)}$	σ_P ($\times 10^{-24}$ cm^2)	Monte Carlo I_{eff} (barns) (res)	(total)	I_{eff} calculated by Bushnell, using Dresner's methods (res)	(total)	$I_{eff(total)}$ by other experiments (barns)
Infinite Dilution								69.8 81.3
0.2439	36.2	38.7±56.6	5981	59,4	61.9	73.37	75.9	
0.3991	37.0	39.5±34.6	3626	63.1	65.6	53.56	56.1	
0.6231	37.6	40.1±22.0	2270	46.8	49.3	35.34	37.8	
0.7370			2000					57.4
0.9013	40.6	43.1±15.2	1506	49.5	52.0	40.95	43.4	

* It should be noted that the uncertainty given for these values is caused by the uncertainty of ± 1 percent in the R.E.P., indicating that one would not normally determine I_{eff}, the "effective resonance integral", from measurements of the R.E.P..

TABLE 7. VALUES USED FOR COMPUTATION OF $\bar{\xi}$

N_{Th}	$_s$(cm^{-1})	ξ_{ox}	N_{ox}	σ_{ox}(b)	$\xi_{ox\ ox}$	ξ_H	N_H	σ_H(b)	$\xi_{H\ H}$	ξ_N	N_N	σ_N(b)	$\xi_{N\ N}$	$\bar{\xi}_s$
0.2439	1.459	0.12	35.42	3.8	0.0162	1	64.99	20.2	1.3128	0.136	0.976	9.1	0.0121	0.9192
0.3991	1.448	0.12	36.69	3.8	0.0167	1	63.81	20.2	1.2890	0.136	1.596	9.1	0.0198	0.9154
0.6231	1.419	0.12	38.91	3.8	0.0177	1	61.43	20.2	1.2409	0.136	2.492	9.1	0.0308	0.9087
0.9013	1.359	0.12	39.64	3.8	0.0181	1	57.64	20.2	1.1643	0.136	3.605	9.1	0.0446	0.9029

N_i = number density of nuclide i ($\times 10^{21}$) per cc.

σ_i = microscopic scattering cross-section of i th nuclide

$\sum_i = N_i\ \sigma_i$

$\sum_s$ = total macroscopic scattering cross-section for all nuclides present

$$\bar{\xi} = \frac{1}{\sum_s(u)} \sum_{i=1}^{N} \xi_i \sum_s^{(i)} (u)$$

Table 8.

W. R. GRACE & COMPANY
Davison Chemical Division
Erwin, Tennessee

CERTIFICATE OF ANALYSIS

Material Thorium Nitrate Solution — Date 8-18-61

Customer Virginia Polytechnic Institute
Virginia Engineering Experimental Station — Date Shipped 8-17-61
Blacksburg, Virginia — Bill of Lading No. 4043

Purchase Order No. A-1007 — Sales Order No. 2130

ELEMENT	ANALYSIS, ppm
Ag	< 0.10
Al	18
B	0.28
Ba	< 5
Be	< 0.1
Bi	4
Ca	34
Cd	< 0.1
Co	< 1
Cr	6
Cu	3
Fe	120
Li	< 50
Mg	12
Mn	< 2
Mo	< 1
Na	< 75
Ni	< 10
P	170
Pb	< 1
Si	10
Sn	2
Sr	< 100
Ti	0.75
V	< 5
Zn	< 25
Zr	< 2

Thorium 406.5 grams/liter

Certified By: K. D. Hensley
Quality Control Department

SINCE
F&R
1881

FROEHLING & ROBERTSON, INC.
INSPECTION ENGINEERS • CHEMISTS • BACTERIOLOGISTS
CABLE ADDRESS "FROEHLING"

MAIN OFFICE AND LABORATORIES
814 WEST CARY STREET
RICHMOND, VIRGINIA
PHONE 644-3021

BRANCH LABORATORIES
NORFOLK, CHARLOTTE, RALEIGH
WASHINGTON, BALTIMORE
GREENVILLE, ROANOKE, WILMINGTON

TABLE 9

RICHMOND, VA.
DECEMBER 27, 1961

NO. J-421-12

ANALYSIS OF 8 AQUEOUS SOLUTIONS OF FERRIC NITRATE

MADE FOR: VIRGINIA POLYTECHNIC INSTITUTE, DEPARTMENT OF PHYSICS,
BLACKSBURG, VA. ATTN: MR. LEE S. ANTHONY,
GRADUATE ASSISTANT

MARKED: AS SHOWN BELOW:

0-0-0

SAMPLE NO.	TOTAL IRON as Fe, % BY VOLUME
E1	3.10
E2	2.96
E3	3.29
E4	8.59
C - CONCENTRATED $Fe(NO_3)_3$	6.30
D - FIRST DILUTION $Fe(NO_3)_3$	3.80
E - SECOND DILUTION TAKEN AFTER FIRST CARBOY	3.12
F - VERY DILUTE $Fe(NO_3)_3$	0.0046

REMARKS: PRELIMINARY TESTS INDICATED THAT THE IRON CONTENT COULD BE DETERMINED BY EITHER OF TWO PROCEDURES, NAMELY, (1) PRECIPITATING THE IRON BY MAKING THE ACIDIFIED SOLUTIONS AMMONIACAL, FILTERING OFF THE R_2O_3, IGNITING AND WEIGHING THE OXIDES GRAVIMETRICALLY; (2) BY REDUCING THE ACIDIFIED SOLUTIONS WITH STANNOUS CHLORIDE AND TITRATING WITH N/20 POTASSIUM DICHROMATE SOLUTION. THE ABOVE RESULTS WERE OBTAINED USING THE LATTER PROCEDURE.

RESPECTFULLY,

FROEHLING & ROBERTSON, INC.

4cc VIRGINIA POLYTECHNIC INSTITUTE

ed

W. R. GRACE & COMPANY
Davison Chemical Division
Erwin, Tennessee

CERTIFICATE OF ANALYSIS

TABLE 10

Material Thorium Nitrate — Date March 6, 1962

Customer Commonwealth of Virginia
Virginia Polytechnic Institute
Blacksburg, Virginia — Date Shipped March 5, 1962

Bill of Lading No. 4247

Purchase Order No. 10508 — Sales Order No. 2263

ELEMENT	ANALYSIS, ppm		
	$Th(NO_3)_4$		
	Container Number	Grams of Thorium per Liter	
1	H-1	277.58	
2	H-2	296.15	First Dilution
3	I-1	396.04	
4	I-2	166.20	Second Dilution
5	G-1	401.97	Concentrated
6	J	0.684	

Certified By: [redacted]
Quality Control Department
K.D. Hensley

ABSTRACT

A determination of the resonance escape probability of thorium as thorium nitrate in aqueous solution has been made as a function of thorium concentration.

The physical system used was an aluminum box surrounded by successive layers of cadmium, paraffin and borated paraffin to keep out neutrons scattered by objects in the laboratory.

Neutrons were obtained from a Cockcroft-Walton type accelerator by the $D(d,n)He^3$ reaction. The drive-in target was located at the center of one of the faces of the aluminum box.

Neutron density was measured at nine spatial positions in the direction of the neutron beam with a bare boron trifluoride detector. The area under a curve of neutron density versus spatial position was obtained for various concentrations of absorber.

The above process was carried out for the thorium solution and for a "mock solution", whose cross-section was similar to that of thorium except that it had no resonances in the thorium resonance region.

By taking ratios of the neutron densities (area under curves of neutron density versus spatial position) in the thorium solution to the neutron density in the mock solution, it was possible to determine the resonance escape probability of neutrons in a homogeneous, aqueous solution of thorium nitrate.

It is shown that, for the absorber concentrations used in this experiment, the resonance escape probability for an infinite

geometry may be obtained by the above ratio method. The difference between a finite system and an infinite one is exhibited as leakage of neutrons from the system in the finite case. If one can compare neutron densities for systems which are large enough so that leakage is negligible or for systems with corresponding leakage rates, the effect of leakage can be overcome and the resonance escape probability for the infinite geometry obtained.

Before taking the above ratios of neutron densities, it was necessary to compensate for the spectral shift of the thermal flux in the two solutions. After such a correction, the resonance escape probability so obtained shows good correlation with the results of the Monte Carlo prediction for this system. Over the range covered by the experiment (0 - 1 x 10^{21} atoms of thorium per cubic centimeter), experimental results agree with Monte Carlo predictions to within one percent.

Counting statistics were good, with 10^6 counts normally taken per spatial position. The curves from which the values of neutron density were determined were formed by nine points, each of which represented at least 10^6 counts. Reproducibility of the neutron density at a point was of the order of one percent. Various changes made in the analysis of the data have caused corresponding changes in the values obtained for the resonance escape probability of less than one percent. These facts all indicate that the uncertainty in the experimental determination is of the order of one percent.

Calculations of effective resonance integrals from the experimentally determined values of the resonance escape probability show good agreement with published measurements on other systems.